HHS Public Access

Author manuscript

Cell Rep. Author manuscript; available in PMC 2026 March 02.

Published in final edited form as:

Cell Rep. 2026 January 27; 45(1): 116759. doi:10.1016/j.celrep.2025.116759.

A prophage-expressed type IV pilus component provides anti-phage defense

Kristina M. Sztanko[1], **Taylor J. Ellison**[2], **Jill Greenlaw**[3], **Tatiana Lenskaia**[1], **P. Nathael Javorčík**[1], **Alexa D. Fitzpatrick**[3], **Karen L. Maxwell**[3], **Courtney K. Ellison**[2], **Alan R. Davidson**[1,3,4,*]

[1]Department of Molecular Genetics, University of Toronto, Toronto, ON M5S 1A8, Canada

[2]Department of Microbiology, University of Georgia, Athens, GA 30602, USA

[3]Department of Biochemistry, University of Toronto, Toronto, ON M5S 1A8, Canada

[4]Lead contact

SUMMARY

Phage genomes integrated within bacterial genomes, known as prophages, frequently encode proteins that provide defense against further phage infection. These proteins often function by altering the cell surface and preventing phages from attaching to their host receptor. Here, we describe prophage-encoded proteins that resemble FimU, a component of the *Pseudomonas aeruginosa* type IV pilus. These phage FimU proteins are incorporated into the pilus without altering its function, yet they mediate robust protection against infection by phages that bind to the tip of the pilus, where FimU is located. The phage FimU proteins and the phage tail proteins that likely interact with FimU are highly diverse, suggesting that evolution in this system is driven by phage versus phage competition. These phage FimU proteins represent an example of anti-phage defense mediated by the replacement of a bacterial cell surface component with a phage-encoded protein.

Graphical Abstract

*Correspondence: alan.davidson@utoronto.ca.

AUTHOR CONTRIBUTIONS

K.M.S. and A.R.D. conceptualized this work. K.M.S., T.J.E., J.G., and C.K.E. performed experiments with assistance from P.N.J. and A.D.F. K.M.S., T.J.E., J.G., C.K.E., and A.R.D. analyzed the data. Bioinformatics were performed by K.M.S., T.L., and A.R.D. K.M.S. and A.R.D. wrote this manuscript with input from K.L.M. and C.K.E. All authors approved the final version and conclusions.

RESOURCE AVAILABILITY

Lead contact

Requests for further information, resources, and reagents should be directed to and will be fulfilled by the lead contact, Alan R. Davidson (alan.davidson@utoronto.ca).

Materials availability

This study did not generate new, unique reagents.

Data and code availability

This paper does not report original code. Raw RNA-seq reads for PAO1 and PAO1 (JBD68) have been deposited at the NCBI Sequence Read Archive under accession SRA: PRJNA1364051 and are publicly available as of the date of publication. Any additional information required to reanalyze the data reported in this paper is available from the lead contact upon request.

DECLARATION OF INTERESTS

The authors declare no competing interests.

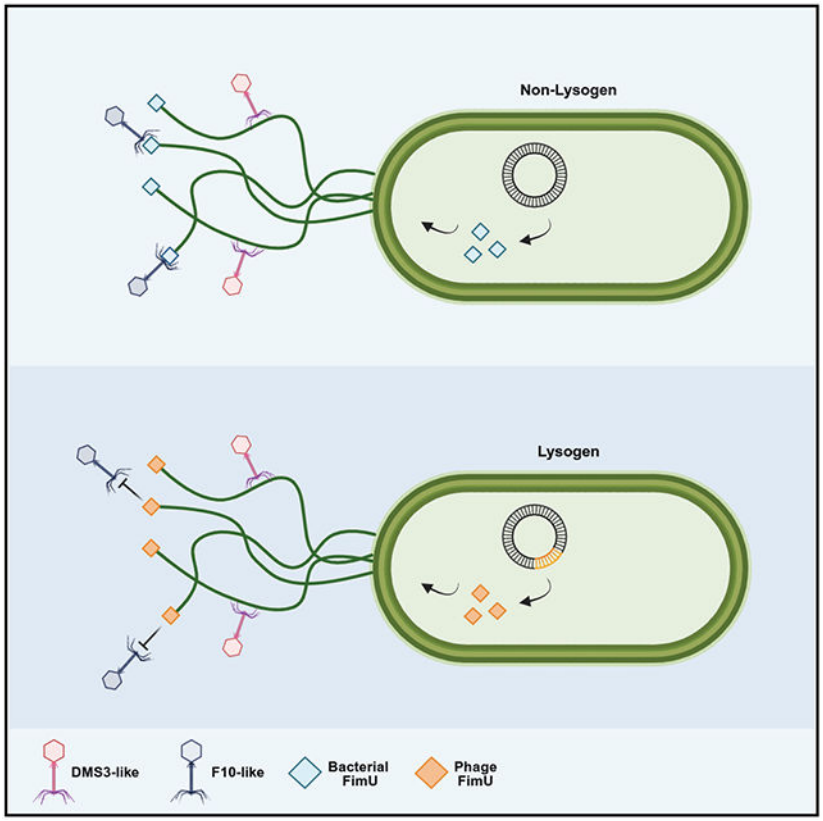

In brief

Sztanko et al. demonstrate that *Pseudomonas aeruginosa* prophages encode proteins resembling the type IV pilus minor pilin protein, FimU. These prophage-expressed FimU proteins are incorporated into the pilus without disrupting pilus function and prevent the adsorption of phages that bind to the tip of the pilus, where FimU is located.

INTRODUCTION

Most bacterial genomes contain integrated phage genomes, which are known as prophages. While prophages can be induced and mediate the formation of viral particles, their frequent persistence within bacterial genomes has led to symbiotic relationships between prophages and their bacterial hosts. An important manifestation of this symbiosis is that prophages generally express genes that provide a fitness advantage to their host.[1] These genes can enhance fitness by many means, frequently by providing defense against infection by other phages. The characterization of prophage-encoded anti-phage defenses has led to the discovery of many novel and intriguing mechanisms to inhibit phage replication.[2-9]

One common way that prophages defend against phage infection is by preventing phage adsorption to the cell surface. For example, phages infecting *Pseudomonas aeruginosa* (*Pae*) almost invariably adsorb to cells by binding lipopolysaccharide (LPS) or the type IV pilus (T4P). The prophage of *Pae* phage D3 produces proteins that alter the LPS, which prevents adsorption by many LPS-dependent phages.[10] Similarly, several different

Pae prophage-produced proteins have been identified that prevent normal T4P function so that phages requiring this structure for adsorption are unable to infect.[2-4,9]

Here, we focus on phages that bind to the T4P. The T4P is a long, thin structure that extends from the surface of the cell and is involved in a variety of processes, including twitching motility.[11] The T4P is largely made up of the major pilin, PilA, which is polymerized and depolymerized to elicit T4P extension and retraction.[11,12] The T4P in *Pae* also contains five minor pilins, PilE, PilX, PilV, PilW, and FimU, which are found in lower abundance and are predicted to be located at the tip of the T4P.[13-16] Finally, *Pae* encodes a T4P adhesin protein, PilY1, which is thought to be involved in surface sensing and epithelial cell adhesion.[17-19] The minor pilin, FimU, which is the focus of this study, is a component of the assembled T4P[13,15] and interacts with the major pilin, PilA, and the minor pilin proteins.[16,20] The minor pilin proteins have been proposed to form an initiation complex required for PilA polymerization. Specifically, FimU and PilE likely act as adaptors to connect the major pilin PilA to the remaining minor pilins and PilY1. In this model, the minor pilins are positioned at the tip of the T4P, with PilA monomers polymerizing underneath the minor pilin complex.[20] Although no structures of the complete T4P have yet been solved to prove this model, many different lines of evidence strongly support it.[13,21-24] The T4P mediates motility by adhering to surfaces through interactions with its tip and then retracting the pilus structure back into the cell. Phages that bind the T4P are likely pulled to the cell surface upon T4P retraction,[14] but the subsequent steps leading to genome injection are not known.

This study investigates a group of T4P-dependent phages related to *Pae* phage JBD68, which we isolated in a previous study.[5,25] These phages, which we refer to as F10-like after the first described phage of this type,[26,27] are united by a very similar set of proteins that comprise their virion structures. They are distinguished from other characterized phages by possessing a unique set of proteins at their tail tip.[25] In this paper, we describe the discovery that F10-like phages express a protein with significant sequence similarity to minor pilin protein FimU (~30% pairwise identity across a 180 amino acid alignment). We show that these phage FimU proteins alter the T4P to defend against phage infection. This defense operates within the context of prophage expression of these proteins but functions only against F10-like phages, not other T4P-dependent phages. We have elucidated the mechanism of this anti-phage defense and have also identified the phage proteins that likely interact with FimU to mediate cell surface attachment. This work describes a previously uncharacterized mechanism for anti-phage defense and suggests that diversity among F10-like phages may be driven by phage versus phage competition.

RESULTS

F10-like phages encode proteins similar to the minor pilin protein, FimU

Through analysis of the genome of the T4P-dependent F10-like phage JBD68, sequenced as part of a previous study in our laboratory,[5] we discovered that it encodes a protein that is similar in sequence to the T4P component, FimU (shares 28% sequence identity with FimU of *Pae* strains PAK and PAO1). The gene encoding this phage FimU protein, referred to as P-FimU, lies within the cluster of genes encoding components of the phage tail, between the tail tube and the tail assembly chaperone (Figure 1A). Other *Pae* F10-like phages in our

collection were also found to encode a P-FimU protein in the same genomic location as JBD68 (Figure 1A). These proteins are similar in amino acid sequence, sharing 70%–99% amino acid sequence identity (Figure 1B). A structure of the JBD68 P-FimU predicted by AlphaFold3[28] overlays with the solved structure of *Pae* strain PAO1 FimU[16] with a root-mean-square deviation (RMSD) of only 2.7 Å over 130 backbone positions (Figure 1C; Table S1).

P-FimU proteins block replication of F10-like phages

Since the F10-like phages and many others are dependent on the T4P for adsorption to the cell surface, we hypothesized that the P-FimU proteins might serve as an anti-phage defense by altering T4P formation. To address this issue, we assessed the effects of P-FimU protein expression on the replication of four different F10-like phages: JBD68, F10, LES2, and LES3. LES2 and LES3 were identified as prophages of the hypervirulent strain LESB58[29,30] and were induced and isolated from this strain. We also tested two pilus-dependent MP22-like phages, DMS3 and D3112,[5] which display no sequence similarity to the F10-like phages in their virion proteins. We spotted serial dilutions of lysates of each phage onto lawns of *Pae* strains expressing the P-FimU proteins from plasmids. We found that each of the four P-FimU proteins tested completely blocked the replication of phages JBD68, F10, and LES3 (Figure 1D). Surprisingly, the replication of phage LES2 was not inhibited by any P-FimU protein, even though most of its virion proteins are highly similar to those of the other F10-like phages, and it encodes a P-FimU protein. The replication of phages DMS3 and D3112 was not affected by the expression of any of the P-FimU proteins, despite these phages also requiring the T4P for adsorption to the cell surface. Replication of all of these phages was blocked by expression of Zip, a prophage-encoded anti-phage defense protein from the phage JBD26 (Gp61), which has been previously shown to block all T4P-dependent phages.[3,9]

To further assess the specificity of P-FimU proteins, we tested four other groups of previously studied, diverse T4P-dependent *Pae* phages. We found that all tested phages were unaffected by expression of P-FimU proteins, but their replication was completely inhibited by expression of Zip (Figure S1A). In summary, these assays showed that P-FimU proteins uniquely blocked F10-like phages that encode them, yet they had no effect on the replication of five other distinct groups of T4P-dependent phages.

P-FimU proteins prevent cell surface adsorption

The predicted structural and sequence similarity of P-FimU proteins to bacterial FimU suggested that P-FimU proteins may be incorporated into the T4P and prevent F10-like phage adsorption. Thus, we sought to determine whether the P-FimU proteins blocked phage adsorption. The standard assay for measuring phage adsorption is to mix phages with cells for varying periods of time and then pellet the cells by centrifugation. Adsorption is detected by titering the supernatant and quantifying the reduction in phage titer resulting from phages binding to the pelleted cells. We found that adsorption of F10-like phages could not be detected by this method, most likely because these phages bind weakly to the cell surface.

As an alternative assay, we cultured phages with cells expressing P-FimU and determined how many phages remained in the culture after varying the incubation times. When phage LES3 was incubated with cells bearing a plasmid expressing the JBD68 P-FimU protein, the titer of phages in the culture remained constant after 18 h of incubation (Figures 1E and S1B). The same behavior was observed when phages were incubated with cells expressing Zip of phage JBD26, which blocks pilus function. By contrast, when phages were mixed with cells expressing the repressor protein of LES3, the phage titer in the culture significantly decreased by more than 10-fold after 18 h (Figures 1E and S1B). In this case, phages adsorb to cells and inject their genomes, but these genomes are subsequently silenced by the repressor so that replication cannot proceed. We conclude that in the cases where P-FimU proteins or Zip was expressed, the titer of phages remains constant in the culture because they are unable to replicate, due to the absence of cell surface adsorption. If replication were blocked in a way that still allowed adsorption and genome injection, as in the case where the LES3 repressor is expressed, the phage titer in the culture would decrease. These data indicate that the JBD68 P-FimU protein, and presumably other P-FimU proteins, prevents adsorption to cells and subsequent injection of the phage DNA.

P-FimU proteins confer anti-phage defense when expressed from prophages

To determine whether the expression of P-FimU proteins by prophages confers resistance to superinfecting phages, phage replication was tested on lysogenic strains bearing JBD68 or LES3 prophages. We found that these prophages did mediate resistance to F10-like phages (Figures 1F and S1C). However, none blocked the replication of phages D3112 and DMS3, indicating that the T4P was still available on the cell surface to act as a receptor for some phages. Phage LES2 was able to form plaques on JBD68 and LES3 lysogens, which is consistent with our observation that plasmid-expressed P-FimU proteins from these phages did not block LES2 replication (Figure 1D). The partially attenuated replication of phage LES2 on the JBD68 lysogen is likely due to the expression of a phage JBD26 Zip homolog that is encoded in the JBD68 genome.

To determine if the resistance mediated by the F10-like prophages was due to P-FimU protein expression, we generated deletions in the genes encoding these proteins in phages JBD68 and LES3. Deleting the gene encoding P-FimU had no effect on the replication of phage JBD68 (Figure S1D). Lysogens bearing these mutant prophages were sensitive to all of the F10-like phages tested except when the infecting phage matched the prophage (Figures 1F and S1C). In these cases, replication was blocked by the prophage-expressed repressor protein, which is required to maintain prophages in an inactive state. The repressor proteins of the F10-like phages used here are diverse in sequence (Figure S2A), so repressor-mediated cross-immunity between these phages was not observed. These data imply that P-FimU proteins are expressed from prophages and that the level of expression is sufficient to inhibit the plaque formation of competing phages.

Transcription level of JBD68 p-fimU gene is similar to that of bacterial fimU

Since we showed that *p-fimU* genes are expressed from prophages, we performed RNA sequencing (RNA-seq) analysis to characterize this transcription. In a *Pae* strain containing a JBD68 prophage, we found that there was no significant difference in the transcription

levels of the *p-fimU* and bacterial *fimU* genes (Figure 2A). Additionally, differential gene expression analysis of the minor pilin genes in lysogenic and non-lysogenic cells showed that there was no significant difference in the transcription of the minor pilin genes or *pilA* in the presence of the JBD68 prophage (Figure 2B). Taken together, these data show that the *p-fimU* and bacterial *fimU* genes are transcribed at similar levels and that transcription of the *p-fimU* gene does not perturb the expression of the other pilin genes. Since the predicted promoter regions of the *p-fimU* genes of the other F10-like phages are almost identical to JBD68 (Figure S2B), the transcriptional regulation of all *p-fimU* genes is likely the same.

P-FimU proteins mediate normal T4P-dependent motility and phage infection

To determine whether the P-FimU proteins can carry out the normal function of bacterial FimU, we introduced the JBD68 P-FimU-expressing plasmid into a *Pae* Δ*fimU* strain. Previous studies showed that Δ*fimU* strains are deficient in T4P-dependent activities, including twitching motility and phage adsorption. Using a standard twitching motility assay,[31] we found that the Δ*fimU* strain containing a plasmid expressing JBD68 P-FimU displayed markedly increased levels of twitching motility compared to the Δ*fimU* strain containing an empty vector (Figure 2C). Furthermore, the levels of twitching mediated by the JBD68 P-FimU were similar to those observed in Δ*fimU* strains expressing the bacterial FimU proteins from strain PAO1 or PA14 (Figure 2C).

Expression of JBD68 P-FimU fully restored the ability of the T4P-dependent phages, DMS3 and D3112, to replicate, as detected in a phage plaque assay, further demonstrating that the P-FimU proteins are able to mediate normal functions of the T4P. The pattern of replication displayed by the F10-like phages on strains complemented by the P-FimU proteins mirrored the results seen when these proteins were expressed in the wildtype strains of *Pae* (Figure 2D). As expected, plasmid-based expression of FimU from strain PAO1 restored the replication of all phages tested, as did the expression of FimU from strain PA14, which shares 45% sequence identity with the PAO1 homolog. It should be noted that phage DMS3 displays some ability to replicate in the PAO1 Δ*fimU* strain, though its replication increased by at least 10-fold in the complemented strains. This is likely due to the presence of some T4P in the Δ*fimU* strain, which also exhibits a low level of twitching.[15] None of the phages tested were able to replicate on the Δ*pilA* strain, which lacks PilA, the major T4P subunit. The ability of Δ*fimU* strains complemented by the JBD68 P-FimU proteins to both support T4P-dependent phage replication and restore twitching motility suggests that P-FimU proteins are incorporated into the T4P.

P-FimU proteins interact with other T4P components and are incorporated into the T4P

To determine whether P-FimU proteins interact with other T4P components in the same manner as bacterial FimU, we performed protein-protein interaction assays using the bacterial adenylate cyclase two-hybrid (BacTH) system.[32] In this assay, proteins are fused to either the T18 or T25 fragments of *B. pertussis* adenylate cyclase and expressed in *E. coli*. Interaction of the fused proteins reconstitutes the cyclase activity, which results in β-galactosidase activity produced from a transcriptional reporter construct. The phage JBD68 P-FimU protein and the *Pae* FimU protein were each fused to the T25 fragment. These proteins were co-expressed with T18 fusions to minor pilin proteins and the major

pilin. As detected through β-galactosidase activity assays, we found that JBD68 P-FimU and PAO1 FimU bound to all of the tested minor pilin proteins and to PilA but did not bind to the pilus motor proteins, PilU and PilB, which were included as negative controls (Figure 3A). The FimU-mediated interactions with pilins observed here are the same as those detected in a previous study using the BacTH system, except that we obtained a positive interaction with PilW, which was not seen before.[16] Overall, the identical behaviors of the phage and bacterial FimU proteins in the BacTH assays support a strong functional similarity between these proteins.

To directly visualize the location of P-FimU proteins in the T4P, we performed immunofluorescence imaging. For this purpose, we used a previously constructed strain that expresses a mutant PilA protein bearing a Cys substitution (A86C). This exposed Cys allows the pilus to be labeled using maleimide dyes.[33-35] This strain also lacks the ATPase needed to retract the T4P (PilT), which increases the number of pili on the surface. Phage JBD68 P-FimU or *Pae* strain PAO1 FimU fused to a triple FLAG tag (3xFLAG) were expressed from plasmids in this strain, allowing these proteins to be visualized using anti-FLAG antibodies. Using fluorescence microscopy, we observed that cells expressing either P-$FimU_{JBD68}$-3xFLAG or Fim_{UPAO1}-3xFLAG possessed similar numbers of pili on their surfaces and that this number did not differ from the strain containing an empty vector (Figure 3B). This result indicated that the expression of the tagged FimU proteins did not affect T4P assembly. We also found that strains expressing tagged bacterial or P-FimU displayed similar levels of immunofluorescence signaling at their cell poles, resulting from anti-FLAG antibody treatment (Figure 3C), showing that both types of FimU were equally incorporated into the T4P. Microscopy images of immunolabeled FimU and maleimide-labeled T4P revealed that FimU localized to the T4P tips in many instances (Figures 3D, S3A, and S3B). This is the predicted localization for minor pilins.[13-16,21-23] The bacterial and phage FimU localized to the cell poles and T4P with similar frequency, demonstrating that P-FimU incorporates into the T4P in the same manner as bacterial FimU. These results also support the hypothesis that P-FimU proteins function by partially replacing bacterial FimU in the T4P to prevent adsorption of F10-like phages. It should be noted that the immunofluorescence procedure can cause shearing of pili, which likely explains why some foci of FimU fluorescence are not localized at cell surfaces.

JBD68 interacts with the tip of the T4P

Since the P-FimU proteins provide protection selectively against the F10-like phages and not other T4P-dependent phages, we surmised that these phages interact with the T4P in a fundamentally different manner from other phages. Previous studies using electron microscopy (EM) to investigate 12 different T4P-dependent *Pae* phages showed that all of them bound along the length of the T4P, suggesting that they interact with the major pilin protein, PilA (Table S2). Protection against the F10-like phages provided by the expression of P-FimU proteins suggests that these phages might interact with bacterial FimU, which is located at the tip of the T4P. To address this issue, we incubated phages JBD68 and DMS3 with *Pae* cells and visualized the phage-T4P interaction using negative-stain transmission EM. We found that phage DMS3, which is not blocked by P-FimU protein expression, bound to varying positions along the T4P shaft, which is composed of the PilA protein

(Figures 4A and 4C). By contrast, the F10-like phage JBD68 exclusively bound to the tip of the T4P (Figures 4B and 4C). This distinct T4P-binding behavior by JBD68, which has not been observed for any other tailed phages, explains why P-FimU proteins, which are also located at the pilus tip, are able to exclusively block the adsorption of F10-like phages and not other T4P-binding phages.

Additional Pae phages encode proteins similar to JBD68 P-FimU

Given the evolutionary advantage that P-FimU proteins could provide, we wondered if homologs of these proteins might be encoded in other phages. BLAST searches initiated using the JBD68 P-FimU protein as a query revealed that many prophages in *Pae* genomes encode P-FimU proteins. The BLAST hits to the P-FimU proteins were found only in F10-like *Pae* prophages, not in other types of *Pae* prophages or prophages in species other than *Pae*. A representative alignment of all the phage-encoded P-FimU proteins found in *Pae* showed that there are five distinct groups of these proteins (Figures S4A and S4B). Groups 4 and 5 contained proteins with high similarity to the JBD68 and F10 P-FimU proteins, respectively. However, groups 1–3 contained P-FimU proteins with distinct sequences. Representatives from each of the three newly discovered groups, named CAAD, BWH, and NSYG, were 45%–76% identical to each other but varied distinctly in sequence from the other P-FimU proteins (20%–32% identity) (Figure S4C). Similarly, the predicted structures of the P-FimU proteins fell into two groups, with the JBD68, F10, LES2, and LES3 structures forming one group (Figure 1C) and the CAAD, BWH, and NSYG P-FimU proteins the other (Figure S4D; Table S1).

We expressed the new P-FimU proteins from a plasmid in *Pae* strains and tested the effect on replication of F10-like phages. Notably, expression of these P-FimU proteins had variable effects. While the JBD68, F10, LES2, and LES3 P-FimU proteins all blocked phages F10, JBD68, and LES3 (Figure 1D), the BWH and NSYG P-FimU proteins blocked only phage JBD68. The CAAD P-FimU protein displayed a unique behavior in being the only one that blocked phage LES2, yet it was unable to block phage LES3 or F10 (Figure 5A). The expression of all of the P-FimU proteins from a plasmid in a *Pae* Δ*fimU* strain restored twitching motility and infection of the T4P-dependent phages DMS3 and D3112 (Figures 5B and S2D). These results show that the P-FimU proteins are generally able to mediate normal T4P function despite their diverse sequences and different effects on phage resistance.

A putative phage tail protein determines inhibition by P-FimU proteins

Since all of the F10-like phages under study here are inhibited by at least one P-FimU protein, they all likely bind to the T4P tip in the vicinity of FimU, as does phage JBD68. However, the F10-like phages also displayed distinct patterns of inhibition by the seven P-FimU proteins tested, implying that there is a variable component of these phage virions that determines their interactions with P-FimU proteins. The virion proteins of phage JBD68 were previously identified through genomic analysis and mass spectrometry of the JBD68 viral particle.[25] The protein products of JBD68 genes 16–24 were found to be virion components of unknown function and are encoded at the 3′ end of the morphogenetic region of the genome, which is where genes encoding tail-tip proteins are usually located in

non-contractile tailed phage genomes.[36] Tail-tip proteins generally determine the cell surface binding properties of phages. Comparison of the sequences of these putative tip proteins (PTPs) among the four F10-like phages used in this study showed that only two of these proteins varied markedly in sequence among these phages (Figures 1A and S5A). One of these proteins, the product of gene *24* in JBD68 (PTP10), was found to be non-essential when a deletion was created in the gene (Figure S5B). Thus, we focused on the other variable tail-tip protein, the product of gene *19*, which we refer to as PTP4 (Figures 1A, S5C, and S5D). Note that we numbered these proteins according to the position of their genes, starting past the gene for the central fiber protein (CFP), which is a conserved, recognizable feature among these phages (Figure 1A).

To determine whether PTP4 was involved in the response to P-FimU-mediated inhibition of replication, we deleted the gene encoding this protein in a JBD68 prophage. Induction of this mutant prophage resulted in the production of no infectious phage particles. We complemented this mutation by expressing the JBD68 PTP4 from a plasmid (referred to as $pPTP4_{JBD68}$) in the same strain (Figure 6A). Phages produced by the complemented prophage replicated robustly on a *Pae* strain containing a plasmid expressing $pPTP4_{JBD68}$ (Figure 6B). Performing the same test in the phage LES3 lysogen showed that the complemented phage was, like wild-type phage JBD68, unable to replicate due to the expression of the LES3 P-FimU protein from the prophage (Figure 6B). We then complemented the JBD68Δ*ptp4* phage with a plasmid expressing the PTP4 homolog from phage LES2 ($PTP4_{LES2}$). This complemented phage replicated robustly on the LES3 lysogen containing a plasmid expressing $PTP4_{LES2}$. Since phage LES2 is not inhibited by P-FimU expressed from the LES3 prophage, these results imply that this resistance to inhibition is mediated by $PTP4_{LES2}$. Collectively, these data suggest that PTP4 is the tail protein that determines the sensitivity of F10-like phages to inhibition by P-FimU proteins.

The role of PTP4 in sensitivity to P-FimU-mediated inhibition is supported by the pattern of phage replication inhibition by the P-FimU proteins (Figures 1D and 5A) as compared to the pairwise sequence identity among the PTP4 proteins (Figure S5D). Phages F10 and LES3 possess identical PTP4 proteins and display identical patterns of inhibition by the P-FimU proteins. Both phages are inhibited by the JBD68, LES3, and F10 P-FimU proteins but not by those from phages BWH, CAAD, and NSYG. The patterns of inhibition of phages JBD68 and LES2 are each distinct from those of the other tested phages, and the sequences of their PTP4 proteins are also unique among these phages.

Other phage genomes encode proteins resembling T4P structural components

Given the effective anti-phage defense provided by the P-FimU proteins, we wondered whether other phages might use similar mechanisms to block phage replication. To address this question, we searched for T4P structural components encoded in other phage and prophage genomes. We performed BLAST searches on a database of phage and bacterial genomes established in our laboratory, in which genes encoding phage-related proteins have been thoroughly annotated.[37] Although this database contains only approximately 750 tailed phage genomes and 2,200 bacterial genomes, we were able to identify one additional example of a T4P component encoded in prophages. In this case, proteins related to the

major T4P subunit, PilA, were encoded in three distinct types of prophages (myophage, siphophage, and podophage) in five different strains of *Xylella fastidiosa* (Figures S6A and S6B). The sequences of these P-PilA proteins fell into two groups that are approximately 50% identical to each other and to the *X. fastidiosa* PilA protein. Predicted structures of these proteins generated by AlphaFold3 could be overlaid on the predicted structure of the *X. fastidiosa* PilA protein with RMSD values below 2 Å (Figure S6C; Table S1).

We also searched the current NCBI database of phage genomes for proteins that resembled T4P components. We found four groups of proteins with sequence similarity to PilA encoded in the genomes of four different types of phages (Table S3). These proteins may function similarly to the P-FimU proteins by incorporating into the T4P and inhibiting phage adsorption. One of these protein families appears to be made up of truncated versions of PilA comprising only the N-terminal 60 residues. This is very unlikely to be a sequencing error, as similar proteins occur in six different *Pseudomonas* phages. During assembly, the conserved N-terminal α helix of PilA monomers is stacked and bundled together to form a hydrophobic core, while variable C-terminal domains are surface exposed.[24] These shorter P-PilA proteins may still be able to incorporate into the T4P but would lack sites of phage binding. Alternatively, it is possible that they may inhibit T4P assembly and prevent T4P-dependent phage infection in this manner. Interestingly, none of the phages encoding the PilA-like proteins are temperate. However, it is well established that virulent phages, such as *E. coli* phage T4, express proteins early in infection that render the infected cells resistant to further superinfection.[38-40] These proteins are presumed to provide an advantage by preventing additional phages from adsorbing to cells that are already infected by the same phage.

DISCUSSION

We have shown here that F10-like prophages produce variant forms of the FimU protein, called P-FimU, that act as molecular mimics, replacing the bacterial FimU proteins with P-FimU proteins that cannot be bound by phages. To our knowledge, this is the first example of phages replacing a bacterial cell surface component with a functional version that is phage resistant. As such, the P-FimU proteins represent a type of prophage-encoded anti-phage system that has not been previously described.

The F10-like phages are, to our knowledge, the first tailed phages to exclusively bind to the tip of the T4P, as shown by our EM experiments (Figure 4). This result suggests that these phages bind to minor pilins that are located at the T4P tip. Several lines of evidence previously implied that FimU and the other minor pilins are positioned at the tip of the T4P,[13-16,21-23] but they have never been directly visualized at the extended pilus tip. Here, we show that both bacterial and phage-encoded FimU proteins are located at the T4P tip by immunofluorescence microscopy. The ability of the P-FimU proteins to incorporate into the T4P was also supported by our demonstration that expression of the P-FimU proteins complemented *Pae ΔfimU* strains with respect to twitching motility (Figures 2C and 5B), and BacTH assays showed that P-FimU and *Pae* FimU interacted with the same minor pilin proteins (Figure 3A). Taking these results together, the simplest explanation for the

inhibitory effect of the P-FimU proteins is that the F10-like phages bind to bacterial FimU but are unable to interact with the P-FimU proteins.

The AlphaFold3-predicted structures of the P-FimU proteins suggest a mechanism for their inhibitory activities. The P-FimU proteins possess large loops and an extended C terminus that are not present in the bacterial FimU protein. These additional regions likely change or occlude the surfaces required for phage binding (Figures 1C and S4D). The P-FimU proteins that have two loops (e.g., F10, JBD68, LES2, and LES3) inhibit more phages (Figures 1D and 5A) than those that have only one loop (e.g., BWH, CAAD, and NSYG). This may indicate different phage binding sites on P-FimU, or it may be that the F10-like phages bind other minor pilins in the T4P tip that are occluded or altered by these P-FimU loops.

Since overexpression of FimU alone has been shown to disrupt pilus assembly,[15] we expected that P-FimU proteins would be expressed at similar levels to the bacterial proteins. Consistent with this idea, the phage *fimU* gene in JBD68 lyso-gens displays similar levels of transcription compared to the bacterial *fimU* (Figure 2A). Additionally, the presence of *p-fimU* does not impact the expression of bacterial *fimU* or the genes encoding the other minor pilins in a lysogen (Figure 2B). Despite the divergence of the P-FimU proteins, the promoter regions upstream of the *p-fimU* genes are over 70% identical, indicating a selective pressure to maintain the appropriate level of transcription consistent with optimal function. Since the transcription of the bacterial and phage *fimU* genes is similar, it is unlikely that the P-FimU proteins completely replace the bacterial FimU proteins when they are expressed from a lysogen. Thus, we suspect that each pilus contains multiple copies of FimU and that the incorporation of one P-FimU within the pilus is sufficient to inhibit the binding of F10-like phages.

We have shown that the PTP4 protein of the F10-like phages determines the sensitivity of a given phage to inhibition by the various P-FimU proteins (Figure 6). Since the sequence of PTP4 determines whether a phage will be blocked by particular P-FimU proteins, we presume that these proteins are also involved in recognizing bacterial FimU proteins. However, PTP4 sequences vary widely between phages, with many pairwise identities at 20% or lower (Figure S5D). By contrast, bacterial FimU proteins vary little in sequence. Through our own searches, we found that *Pae* strains display only two FimU sequence variants: one matching FimU found in PAO1 and the other matching PA14 (45% sequence identity to PAO1). Both of these *Pae* FimU proteins support the replication of all of the tested F10-like phages (Figure 2D). The disconnect between PTP4 and bacterial FimU proteins with respect to sequence diversity leads us to speculate that the diversification of PTP4 sequences results from competitive pressure exerted by P-FimU proteins, which are also very diverse (Figure S4). In other words, this aspect of the evolution of these phages may be driven much more by phage versus phage competition rather than phage versus host. In contrast to *Pae* FimU, the sequences of PilA proteins across *Pae* strains are much more diverse,[41] most likely a result of this major T4P subunit being targeted by many diverse phages. In this case, PilA diversity appears to be driven by direct phage-host competition. Overall, it appears that the F10-like phage precursors may have gained an initial evolutionary advantage by targeting FimU, which is not targeted by other phages.

However, this new niche was subsequently narrowed by interphage competition mediated by the P-FimU proteins.

In summary, this work elucidates a mechanism by which phages express a phage receptor component as a means to block subsequent phage infections. Although this is the first described example of such a mechanism, our identification of T4P components encoded in other diverse phages suggests that this may be a widely employed method of anti-phage defense.

Limitations of this study

A limitation of this study is the unresolved mechanism of P-FimU incorporation into the T4P. It remains unclear how many copies of P-FimU are incorporated into the T4P to sufficiently prevent F10-like phage adsorption, given that P-FimU and bacterial FimU genes share similar transcription levels. Further work is required to understand the regulation of P-FimU expression and the interplay between bacterial FimU and P-FimU during incorporation into the T4P. In addition, structural modeling and mutagenesis could elucidate the mechanisms allowing P-FimU proteins to be functional for twitching motility but unable to bind F10-like phages.

STAR★METHODS

EXPERIMENTAL MODEL AND STUDY PARTICIPANT DETAILS

Microbes: *Pseudomonas aeruginosa* strains (PAO1, PAK and mutant derivatives PAO1 Δ*pilT*,[42] PAO1 Δ*fimU*,[16] PAO1 Δ*pilA*,[42] PAO1 *pilA* A86C, *pilT*::Tn5,[21] PAO1 I-C CRISPR,[43] PAO1 I-C CRISPR *Δhel*, PAK (LES3 Δ*p-fimU*) and PAK (JBD68 Δ*p-fimU*)) and *Escherichia coli* strains (DH5α, SM10 λpir and BTH101) were cultured at 37°C, or 30°C when appropriate, in lysogeny broth (LB) or on LB agar supplemented with antibiotics at the following concentrations when appropriate: ampicillin, 100 μg/mL for *E. coli*; kanamycin, 30 μg/mL for *E.coli*; gentamicin, 30 μg/mL for *E. coli* and 50 μg/mL for *P. aeruginosa*.

Phages: *Pseudomonas aeruginosa* phages (JBD68, F10, LES2, LES3, DMS3, D3112, M6, F116, Luz19, AB05, ΦKMV, ΦKMZ) and mutant phages (JBD68 Δ*p-fimU,* JBD68 Δ*ptp4*, JBD68 Δ*ptp10 and LES3* Δ*p-fimU)* were propagated on either PAO1 or PAK and stored in SM buffer (100 mM NaCl, 8 mM Mg2SO4, 50 mM Tris-HCl pH 7.5) at 4°C.

METHOD DETAILS

Bioinformatics: Phage-encoded pilus proteins were identified using BLAST[52] searches. Clinker[47] was used to generate genomic maps of F10-like phages and all other prophages in this study. Multiple sequence alignments were generated in Jalview Version 2[48] using MUSCLE[53] with default settings. Pairwise alignment percent identities were also generated using Jalview Version 2. Predicted structures were generated using AlphaFold3,[28] proteins overlays were generated using Pymol 2.5.3[50] and RMSD scores were generated using DALI.[49] Figure 6A was created in BioRender (Maxwell, K. (2025) https://BioRender.com/w50y291 agreement number KB290BY7B3). Promoters were predicted using Promoter

Calculator algorithm by De Nova DNA.[51] A list of all relevant accession numbers can be found in Table S4.

Bacterial strains and plasmids: Strains, phages and plasmids used in this work are detailed in the Key Resources table. When phage F10 was required, *Pae* strain PAK was used as this strain is susceptible to F10. Otherwise, strain PAO1 was used because required mutants were already available in this strain. Strains PAO1 and PAK encode the same type of T4P and their FimU proteins are identical. Strains were grown in 3 mLor 5 mL of Lysogeny broth (LB) or on 1.5% LB agar plates for 18 h (overnight) at 37°C unless otherwise stated. *Pae* strains were transformed with plasmids using electroporation and chemically competent *Escherichia coli* as previously described.[54] When required, media was supplemented with 50 μg/mL or 30 μg/mL gentamicin for *Pae* and *E. coli,* respectively. Expression from the pBAD promoter on high copy number plasmid, pHERD30T, was induced with 5 mM L-arabinose where indicated. The type I-C CRISPR-Cas system expressed in strain PAO1 was induced with 0.5 mM isopropylβ-D-1 thiogalactopyranoside (IPTG).

DNA cloning and manipulation: Lysogens of JBD68, F10 and LES3 were used for amplification of *p-fimU* genes using PCR. BWH, CAAD & NSYG *P-fimU* genes were synthesized by Twist Bioscience, South San Francisco, California, USA. All genes were cloned into pHERD30T using the restriction enzymes, NcoI & HindIII. Spacers targeting LES3 and JBD68 *p-fimU* were cloned into pHERD30T using the restriction enzyme BsaI.[43] All cloning and mutagenesis was confirmed via sequencing performed by The Center for Applied Genomics, The Hospital for Sick Children, Toronto, Canada.

Small deletions in the phage genes encoding P-FimU proteins were created using an I-C CRISPR-Cas system bearing a helicase-attenuated mutant Cas3 protein.[43,55] Strain PAO1 harboring the mutant I-C CRISPR system was grown to OD_{600} = 0.4 at 37°C. Phage was added at an MOI of 10 and grown at 37°C for 18 h. Phage lysates were collected as described below. *P-fimU* mutants were isolated by performing phage plaquing assays (described below) on PAO1 with an integrated I-C CRISPR system containing the wild-type helicase to facilitate efficient selection against wild-type phage. The resulting plaques were isolated in SM buffer and mutations were confirmed via PCR and DNA sequencing. Deletions in the JBD68 gene encoding PTP10 were made in the same manner.

A deletion mutant of JBD68 *ptp4* was generated using a deletion construct in pEX18Gm[45] to remove the region between nucleotides 16262–17162. 500 nucleotide homology arms were used to facilitate homologous recombination to result in an in-frame, internal deletion of amino acids 80–380 of JBD68 PTP4. pEX18Gm constructs were transformed into SM10 *E. coli* for mating into *Pae* strain PAO1 (JBD68). Mutants were confirmed via PCR and DNA sequencing. All bacterial strains and oligonucleotides used in this study are summarized in Key Resources table.

Phage lysate production and lysogen formation: Phage lysates were produced by growing lysogens at 37°C overnight, allowing spontaneous prophage production. Overnight cultures were centrifuged for 2 min at 10,000 X *g* and the supernatant was collected. A

few drops of chloroform were added to the supernatant and incubated for 30 min at room temperature, with rocking. Lysates were centrifuged one final time (10,000 X *g*, 10 min) to remove cell debris and stored at 4°C. Phage lysates were normalized to 10^8–10^{10} PFU/mL.

Lysogens were isolated by plating 10-fold serial dilutions of phage lysate on either PAO1 or PAK. Cells from the center of zones of clearing streaked to single colonies and then streaked across their respective lysates to identify resistant colonies. Resistant colonies were then confirmed as lysogens by growing the putative lysogens at 37°C overnight, collecting the supernatant, and plating the lysates on their respective host strains to confirm infectious phage particles were produced.

Phage plaquing assays: Phage plaquing assays were performed as previously described with minor modifications.[54] 200 μL of overnight *P. aeruginosa* culture was added to 3 mL of 0.6% LB agar and top plated on a 1.5% agar plate containing 10 mM MgSO4 and, when necessary, 50 μg/mL gentamicin and 5 mM arabinose (expression from pHERD30T). Phage lysates were 10-fold serial diluted in SM buffer (100 mM NaCl, 8 mM $MgSO_4$ & 50 mM Tris-HCl (pH 7.5)) and spotted on the surface. Plates were incubated at 30°C overnight. All spotting assays were repeated at least 3 times with high reproducibility. Data shown in figures depict one representative experiment.

Phage adsorption assays: Cells were grown to an OD_{600} of 0.5 in LB supplemented with 5 mM arabinose to induce expression of proteins from the plasmid. Phage lysates were added at an MOI of 0.1 and incubated for 0, 5, 8 or 18 h. At each time point a supernatant aliquot was taken and centrifuged at 10,000 x g for 2 min. The supernatant was then transferred to a new tube and incubated at room temperature with chloroform for 20 min, with rocking. Lysates were centrifuged a final time (10,000 xg for 10 min) and 10-fold serial dilutions were prepared and spotted on a sensitive lawn as described above (see phage plaquing assays). Phage titers were quantified by plating dilutions of lysate in triplicate on a sensitive lawn. 10 μL of diluted phage lysate were mixed with 200 μL of overnight culture in 3 mL of 0.6% top agar and incubated at 30°C overnight. Plaques were counted and averaged across triplicates and the titer was calculated. This was repeated for three biological replicates. Titers were normalized to the 0 h timepoint (input) and an unpaired two-tailed Student's *t* test comparing phage titers normalized to input at 0 h and 18 h was performed using GraphPad Prism version 9.0.1 for Mac, GraphPad Software, Boston, Massachusetts USA, www.graphpad.com.

Twitching motility assays: Twitching motility assays were performed as previously described[31] with the following modifications. Individual colonies were stabbed into 1% LB agar (1% agar, 1% tryptone powder, 0.5% yeast extract & 0.5% NaCl) supplemented with gentamicin and arabinose and poured in pre-treated tissue culture-grade plates (VWR). Three replicates were performed with a minimum of three colonies per replicate. Plates were incubated at 37°C for 24 h, inverted. The agar was then removed, and the plates were stained with 1% crystal violet for 5 min while shaking. Excess stain was washed away with distilled water. Stained twitching areas were measured manually and Ordinary One-way ANOVA with multiple comparisons was performed using GraphPad Prism version 9.0.1 for Mac, GraphPad Software, Boston, Massachusetts USA, www.graphpad.com.

Bacterial adenylate two-hybrid (BACTH) assays: Bacterial adenylate cyclase two-hybrid assays were performed as previously described.[31] Genes encoding the P-FimU proteins from JBD68 and F10 and *fimU* from PAO1 were cloned into pKT25 (T25) using standard restriction enzyme cloning methods. Similarly, the minor pilin genes *pilE*, *pilV*, *pilX*, *pilW*, as well as *pilA*, *pilU* and *pilB* were cloned into pUT18C (T18). Plasmids were co-transformed into *E. coli* BTH101 Δ*cya* and triplicate single colonies were grown overnight and 30°C in LB supplemented with kanamycin 30 μg/mL and ampicillin 100 μg/mL. 3 μL of overnight culture was spotted in triplicate onto MacConkey agar (1.5% agar, 30 μg/mL kanamycin, 100 μg/mL ampicillin, 0.5 mM IPTG and 1% maltose) as well as LB X-gal plates (1.5% agar, 30 μg/mL kanamycin, 100 μg/mL ampicillin, 0.5 mM IPTG and 40 μg/mL X-gal). Plates were incubated at 30°C overnight.

Fluorescence microscopy to visualize P-FimU: pHERD30T plasmids carrying FimU-3xFLAG alleles were introduced by electroporation into a previously published strain of *P. aeruginosa* containing a pilin cysteine knock-in for maleimide-T4P labeling and a retraction motor *pilT*::Tn5 insertion to produce non-retractile T4P for optimal visualization.[33] Cells were immunolabeled and their T4P were labeled as described previously with some species-specific modifications.[35,56] 100 μL of overnight cultures of *P. aeruginosa* strains carrying pHERD-FimU expression constructs were spotted onto LB plates containing gentamicin (30 μg/mL) and grown at 37°C for 4 h. Plate-grown cells were then scooped off of plates using a P200 pipette tip and resuspended into 100 μL LB medium. Cells were then incubated with 50 μg/mL AF488-maleimide (Invitrogen) in the dark at room temperature for 45 min to 1 h. Cells were then washed once with 200 μL LB and then fixed by resuspension in 100 μL of LB containing 4% paraformaldehyde (Electron Microscopy Sciences) and incubation in the dark for 15 min. Fixed cells were washed once with 200 μL LB and resuspended in 50 μL 0.05% Tween 20 in phosphate-buffered saline (PBST) containing 1:100 dilution of mouse α-FLAG antibody (Sigma) and incubated overnight with end-over-end rotation at 4°C. Cells were then washed three times using 200 μL PBST and resuspended in 100 μL PBST containing 1:200 dilution of goat α-mouse-AF555 and incubated for 2 h with end-over-end rotation at 4°C. Cells were then washed three times with 200 μL PBST and then washed once more with 200 μL of PBS and resuspended into a final volume of 200 μL PBS (to remove background fluorescence from the Tween 20) before imaging under a 1% agarose PBS pad. All centrifugation during wash steps was carried out at 12,000 x *g* for 1 min. Cell bodies were imaged using phase-contrast microscopy while labeled T4P and immunolabeled FimU were imaged using fluorescence microscopy on a Nikon Ti2-E microscope using a Plan Apo 100× oil immersion objective, a GFP/FITC/Cy2 filter set for pili, a dsRed/TRITC/Cy3 Filter Set for immunolabeled FimU, a Hamamatsu ORCA402 Fusion Gen-III cCMOS camera, and Nikon NIS Elements Imaging Software. Representative microscopy images were prepared by first removing the background fluorescence from images using the standard Subtract Background function in Fiji. Notably, populations of *P. aeruginosa* containing labeled T4P exhibit variability in labeling efficiency for unknown reasons. Therefore, immunolabeling fluorescence signal contrast for all images was normalized, but T4P fluorescence signal contrast was adjusted so that T4P were clearly visible for each cell. Cells were quantified manually using the Fiji Cell Counter plugin. Statistics were determined using Prism software version 10.2.1. The percent

of cells with piliation was assessed by counting the number of cells that had T4P present using a commonly applied method.[34] The number of cell counted per sample is included in Table S5.

RNA-seq analysis: Overnight cultures of PAO1 and JBD68 lysogens were subcultured 1:100 in fresh LB and grown at 37°C to late log phase. Cells were pelleted by centrifugation and flash frozen. All the RNA samples were sequenced by an external provider (SeqCenter, Pittsburgh PA USA) following the rRNA depletion approach and using Illumina's Stranded Total RNA Prep with Ribo-Zero Plus Microbiome kit to generate unbiased high-quality RNA libraries. The sequencing process utilized a NovaSeq X Plus, yielding 150 bp paired-end reads and 12M Paired End Reads (1.8 Gbp) per sample. Demultiplexing, quality assessment, and adapter trimming were completed using bcl-convert (v4.2.4). The data quality checks for all the FASTQ files were conducted to evaluate overall data quality and determine whether any additional preprocessing steps were necessary (e.g., to filter out low-quality reads and to trim the adapter sequences). Table S6 contains the descriptive statistics. We did the quality checks using FastQC. In addition, strandness of the RNA-seq data was evaluated. Reads were aligned to the corresponding reference genomes, *Pseudomonas aeruginosa PAO1* (NC_002516.2) and JBD68 (KY707339.1), using minimap2 with default parameters. The overall quality of the resulting alignments was evaluated using IGV. A gene count matrix was calculated using feature Counts. Differential gene expression analysis was conducted using DESeq2.

Transmission electron microscopy: Samples were prepared by resuspending a single colony of PAO1Δ*pilT* (this mutant strain was used because increased numbers of T4P accumulate on the surface of this strain) in 20 μL of SM buffer. 10 μL of cell mixture was incubated with approximately 10^8 phages for 30 min at room temperature. Alternatively, overnight cultures of PAO1 Δ*pilT* were subcultured and grown to approximately OD_{600} = 0.7. Cells were diluted 10-fold in SM buffer and 10 μL of this mixture were incubated with approximately 10^8 phages for 30 min at room temperature. Samples were allowed to bind to glow-discharged carbon grids for 2 min. Samples were washed twice with double distilled water and stained with 2% uranyl acetate for 15 s. Dried grids were imaged on Talos L120C transmission electron microscope (Microscopy Imaging Laboratory, Faculty of Medicine, University of Toronto, Toronto, Canada). Phages bound at tip versus not at tip were counted (minimum 100 particles per sample) and an unpaired two-tailed Student's *t* test comparing phages bound at the tip and not at tip for both DMS3 and JBD68 was performed using GraphPad Prism version 9.0.1 for Mac, GraphPad Software, Boston, Massachusetts USA, www.graphpad.com.

F10-like PTP4 complementation assays: A single colony of PAO1 (JBD68 Δ*ptp4*) harboring pHERD30T expressing either $PTP4_{JBD68}$, $PTP4_{LES2}$ or empty vector were grown in 5 mL of LB supplemented with gentamicin and arabinose overnight. The following day, 2 mL of lysate were prepared as described above. 10-fold serial dilutions of prepared lysates were spotted as described above on lawns of PAO1 harboring the same pHERD30T vector used to complement JBD68 Δ*ptp4.* Plates were incubated at 30°C overnight. Note that sufficient complementation required expression of the upstream gene (JBD68 ARM70480.1

& ARM70481.1[PTP4$_{JBD68}$] and LES2 WP_010791962.1 & WP_010791961[PTP4$_{LES2}$]) as expression of just *ptp4* from either phage did not allow for robust replication, likely due to a stoichiometric requirement between the two gene products.

QUANTIFICATION AND STATISTICAL ANALYSIS

All experiments, with the exception of RNA-seq, were performed with at least three biological replicates ($n = 3$). Statistical parameters are reported in the figure legends and method details.

Supplementary Material

Refer to Web version on PubMed Central for supplementary material.

ACKNOWLEDGMENTS

The authors thank Lori Burrows and members of the Davidson and Maxwell laboratories for their helpful discussions. This study was supported by grants from the Canadian Institutes of Health Research to K.L.M. (PJT-165936) and A.R.D. (FDN-15427), a grant from the National Institutes of Health awarded to C.K.E. (R35GM150916), and a Natural Sciences and Engineering Research Council Arthur B. McDonald Fellowship to K.L.M. (SMFSU-581368-2023). C.K.E. is a Damon Runyon-Marilyn and Scott Urdang Breakthrough Scientist supported by the Damon Runyon Cancer Research Foundation (DFS6023). A.R.D. is the Canada Research Chair in Bacteriophage-Based Technologies (CRC-2024-00209). K.L.M. is the Canada Research Chair in Bacteriophage Biology and Therapeutics (CRC-2023-00010).

REFERENCES

1. Brüssow H, Canchaya C, and Hardt W-D (2004). Phages and the Evolution of Bacterial Pathogens: from Genomic Rearrangements to Lysogenic Conversion. Microbiol. Mol. Biol. Rev 68, 560–602. 10.1128/MMBR.68.3.560-602.2004. [PubMed: 15353570]
2. Chung I-Y, Jang H-J, Bae H-W, and Cho Y-H (2014). A phage protein that inhibits the bacterial ATPase required for type IV pilus assembly. Proc. Natl. Acad. Sci. USA 111, 11503–11508. 10.1073/pnas.1403537111. [PubMed: 25049409]
3. Tsao Y-F, Taylor VL, Kala S, Bondy-Denomy J, Khan AN, Bona D, Cattoir V, Lory S, Davidson AR, and Maxwell KL (2018). Phage Morons Play an Important Role in Pseudomonas aeruginosa Phenotypes. J. Bacteriol 200, e00189–18. 10.1128/JB.00189-18. [PubMed: 30150232]
4. Shah M, Taylor VL, Bona D, Tsao Y, Stanley SY, Pimentel-Elardo SM, McCallum M, Bondy-Denomy J, Howell PL, Nodwell JR, et al. (2021). A phage-encoded anti-activator inhibits quorum sensing in Pseudomonas aeruginosa. Mol. Cell 81, 571. 10.1016/j.molcel.2020.12.011. [PubMed: 33412111]
5. Bondy-Denomy J, Qian J, Westra ER, Buckling A, Guttman DS, Davidson AR, and Maxwell KL (2016). Prophages mediate defense against phage infection through diverse mechanisms. ISME J. 10, 2854–2866. 10.1038/ismej.2016.79. [PubMed: 27258950]
6. Uc-Mass A, Loeza EJ, de la Garza M, Guarneros G, Hernández-Sánchez J, and Kameyama L (2004). An orthologue of the cor gene is involved in the exclusion of temperate lambdoid phages. Evidence that Cor inactivates FhuA receptor functions. Virology 329, 425–433. 10.1016/j.virol.2004.09.005. [PubMed: 15518820]
7. Piel D, Bruto M, Labreuche Y, Blanquart F, Goudenège D, Barcia-Cruz R, Chenivesse S, Le Panse S, James A, Dubert J, et al. (2022). Phage-host coevolution in natural populations. Nat. Microbiol 7, 1075–1086. 10.1038/s41564-022-01157-1. [PubMed: 35760840]
8. Rousset F, Depardieu F, Miele S, Dowding J, Laval A-L, Lieberman E, Garry D, Rocha EPC, Bernheim A, and Bikard D (2022). Phages and their satellites encode hotspots of antiviral systems. Cell Host Microbe 30, 740–753.e5. 10.1016/j.chom.2022.02.018. [PubMed: 35316646]

9. Taylor VL, Patel PH, Shah M, Yusuf A, Burk CM, Sztanko KM, Gitai Z, Davidson AR, Koch MD, and Maxwell KL (2025). Prophages block cell surface receptors to preserve their viral progeny. Nature 644, 1049–1057. 10.1038/s41586-25-09260-z. [PubMed: 40670790]
10. Newton GJ, Daniels C, Burrows LL, Kropinski AM, Clarke AJ, and Lam JS (2001). Three-component-mediated serotype conversion in Pseudomonas aeruginosa by bacteriophage D3. Mol. Microbiol 39, 1237–1247. 10.1111/j.1365-2958.2001.02311.x. [PubMed: 11251840]
11. Craig L, Pique ME, and Tainer JA (2004). Type IV pilus structure and bacterial pathogenicity. Nat. Rev. Microbiol 2, 363–378. 10.1038/nrmicro885. [PubMed: 15100690]
12. Jin F, Conrad JC, Gibiansky ML, and Wong GCL (2011). Bacteria use type-IV pili to slingshot on surfaces. Proc. Natl. Acad. Sci. USA 108, 12617–12622. 10.1073/pnas.1105073108. [PubMed: 21768344]
13. Treuner-Lange A, Chang Y-W, Glatter T, Herfurth M, Lindow S, Chreifi G, Jensen GJ, and Søgaard-Andersen L (2020). PilY1 and minor pilins form a complex priming the type IVa pilus in Myxococcus xanthus. Nat. Commun 11, 5054. 10.1038/s41467-020-18803-z. [PubMed: 33028835]
14. Jacobsen T, Bardiaux B, Francetic O, Izadi-Pruneyre N, and Nilges M (2020). Structure and function of minor pilins of type IV pili. Med. Microbiol. Immunol 209, 301–308. 10.1007/s00430-19-00642-5. [PubMed: 31784891]
15. Giltner CL, Habash M, and Burrows LL (2010). Pseudomonas aeruginosa minor pilins are incorporated into type IV pili. J. Mol. Biol 398, 444–461. 10.1016/j.jmb.2010.03.028. [PubMed: 20338182]
16. Nguyen Y, Sugiman-Marangos S, Harvey H, Bell SD, Charlton CL, Junop MS, and Burrows LL (2015). Pseudomonas aeruginosa Minor Pilins Prime Type IVa Pilus Assembly and Promote Surface Display of the PilY1 Adhesin. J. Biol. Chem 290, 601–611. 10.1074/jbc.M114.616904. [PubMed: 25389296]
17. Orans J, Johnson MDL, Coggan KA, Sperlazza JR, Heiniger RW, Wolfgang MC, and Redinbo MR (2010). Crystal structure analysis reveals Pseudomonas PilY1 as an essential calcium-dependent regulator of bacterial surface motility. Proc. Natl. Acad. Sci. USA 107, 1065–1070. 10.1073/pnas.0911616107. [PubMed: 20080557]
18. Heiniger RW, Winther-Larsen HC, Pickles RJ, Koomey M, and Wolfgang MC (2010). Infection of human mucosal tissue by Pseudomonas aeruginosa requires sequential and mutually dependent virulence factors and a novel pilus-associated adhesin. Cell. Microbiol 12, 1158–1173. 10.1111/j.1462-5822.2010.01461.x. [PubMed: 20331639]
19. Bohn Y-ST, Brandes G, Rakhimova E, Horatzek S, Salunkhe P, Munder A, van Barneveld A, Jordan D, Bredenbruch F, Häussler S, et al. (2009). Multiple roles of Pseudomonas aeruginosa TBCF10839 PilY1 in motility, transport and infection. Mol. Microbiol 71, 730–747. 10.1111/j.1365-2958.2008.06559.x. [PubMed: 19054330]
20. Nguyen Y, Harvey H, Sugiman-Marangos S, Bell SD, Buensuceso RNC, Junop MS, and Burrows LL (2015). Structural and functional studies of the Pseudomonas aeruginosa minor pilin, PilE. J. Biol. Chem 290, 26856–26865. 10.1074/jbc.M115.683334. [PubMed: 26359492]
21. Ellison CK, Dalia TN, Vidal Ceballos A, Wang JC-Y, Biais N, Brun YV, and Dalia AB (2018). Retraction of DNA-bound type IV competence pili initiates DNA uptake during natural transformation in Vibrio cholerae. Nat. Microbiol 3, 773–780. 10.1038/s41564-018-0174-y. [PubMed: 29891864]
22. Korotkov KV, and Hol WGJ (2008). Structure of the GspK–GspI–GspJ complex from the enterotoxigenic Escherichia coli type 2 secretion system. Nat. Struct. Mol. Biol 15, 462–468. 10.1038/nsmb.1426. [PubMed: 18438417]
23. Winther-Larsen HC, Wolfgang MC, van Putten JPM, Roos N, Aas FE, Egge-Jacobsen WM, Maier B, and Koomey M (2007). Pseudomonas aeruginosa Type IV pilus expression in Neisseria gonorrhoeae: effects of pilin subunit composition on function and organelle dynamics. J. Bacteriol 189, 6676–6685. 10.1128/JB.00407-07. [PubMed: 17573479]
24. McCallum M, Burrows LL, and Howell PL (2019). The Dynamic Structures of the Type IV Pilus. Microbiol. Spectr 7. 10.1128/mi-crobiolspec.PSIB-0006-2018.

25. Harvey H, Bondy-Denomy J, Marquis H, Sztanko KM, Davidson AR, and Burrows LL (2018). Pseudomonas aeruginosa defends against phages through type IV pilus glycosylation. Nat. Microbiol 3, 47–52. 10.1038/s41564-017-0061-y. [PubMed: 29133883]
26. Lindberg RB, and Latta RL (1974). Phage Typing of Pseudomonas aeruginosa: Clinical and Epidemiologic Considerations. J. Infect. Dis 130, S33–S42. [PubMed: 4213792]
27. Sepúlveda-Robles O, Kameyama L, and Guarneros G (2012). High Diversity and Novel Species of Pseudomonas aeruginosa Bacteriophages. Appl. Environ. Microbiol 78, 4510–4515. 10.1128/AEM.00065-12. [PubMed: 22504803]
28. Jumper J, Evans R, Pritzel A, Green T, Figurnov M, Ronneberger O, Tunyasuvunakool K, Bates R, ZŽídek A, Potapenko A, et al. (2021). Highly accurate protein structure prediction with AlphaFold. Nature 596, 583–589. 10.1038/s41586-021-03819-2. [PubMed: 34265844]
29. Winstanley C, Langille MGI, Fothergill JL, Kukavica-Ibrulj I, Paradis-Bleau C, Sanschagrin F, Thomson NR, Winsor GL, Quail MA, Lennard N, et al. (2009). Newly introduced genomic prophage islands are critical determinants of in vivo competitiveness in the Liverpool Epidemic Strain of Pseudomonas aeruginosa. Genome Res. 19, 12–23. 10.1101/gr.086082.108. [PubMed: 19047519]
30. James CE, Fothergill JL, Kade H, Hall AJ, Cottell J, Brockhurst MA, and Winstanley C (2012). Differential infection properties of three inducible prophages from an epidemic strain of Pseudomonas aeruginosa. BMC Microbiol. 12, 216. 10.1186/1471-2180-12-216. [PubMed: 22998633]
31. Marko VA, Kilmury SLN, MacNeil LT, and Burrows LL (2018). Pseudomonas aeruginosa type IV minor pilins and PilY1 regulate virulence by modulating FimS-AlgR activity. PLoS Pathog. 14, e1007074. 10.1371/journal.ppat.1007074. [PubMed: 29775484]
32. Battesti A, and Bouveret E (2012). The bacterial two-hybrid system based on adenylate cyclase reconstitution in Escherichia coli. Methods 58, 325–334. 10.1016/j.ymeth.2012.07.018. [PubMed: 22841567]
33. Koch MD, Fei C, Wingreen NS, Shaevitz JW, and Gitai Z (2021). Competitive binding of independent extension and retraction motors explains the quantitative dynamics of type IV pili. Proc. Natl. Acad. Sci. USA 118, e2014926118. 10.1073/pnas.2014926118. [PubMed: 33593905]
34. Ellison CK, Kan J, Dillard RS, Kysela DT, Ducret A, Berne C, Hampton CM, Ke Z, Wright ER, Biais N, et al. (2017). Obstruction of pilus retraction stimulates bacterial surface sensing. Science 358, 535–538. 10.1126/science.aan5706. [PubMed: 29074778]
35. Ellison TJ, and Ellison CK (2025). Improved DNA binding to a type IV minor pilin increases natural transformation. Nucleic Acids Res. 53, gkaf467. 10.1093/nar/gkaf467. [PubMed: 40444634]
36. Davidson AR, Cardarelli L, Pell LG, Radford DR, and Maxwell KL (2012). Long noncontractile tail machines of bacteriophages. Adv. Exp. Med. Biol 726, 115–142. 10.1007/978-1-4614-0980-9_6. [PubMed: 22297512]
37. Büttner CR, Wu Y, Maxwell KL, and Davidson AR (2016). Baseplate assembly of phage Mu: Defining the conserved core components of contractile-tailed phages and related bacterial systems. Proc. Natl. Acad. Sci. USA 113, 10174–10179. 10.1073/pnas.1607966113. [PubMed: 27555589]
38. Lu MJ, and Henning U (1994). Superinfection exclusion by T-even-type coliphages. Trends Microbiol. 2, 137–139. 10.1016/0966-842x(94)90601-7. [PubMed: 8012757]
39. Decker K, Krauel V, Meesmann A, and Heller KJ (1994). Lytic conversion of Escherichia coli by bacteriophage T5: blocking of the FhuA receptor protein by a lipoprotein expressed early during infection. Mol. Microbiol 12, 321–332. 10.1111/j.1365-2958.1994.tb01020.x. [PubMed: 8057856]
40. Abedon ST (2019). Look Who's Talking: T-Even Phage Lysis Inhibition, the Granddaddy of Virus-Virus Intercellular Communication Research. Viruses 11, 951. 10.3390/v11100951. [PubMed: 31623057]
41. Giltner CL, Nguyen Y, and Burrows LL (2012). Type IV Pilin Proteins: Versatile Molecular Modules. Microbiol. Mol. Biol. Rev 76, 740–772. 10.1128/MMBR.00035-12. [PubMed: 23204365]

42. Jacobs MA, Alwood A, Thaipisuttikul I, Spencer D, Haugen E, Ernst S, Will O, Kaul R, Raymond C, Levy R, et al. (2003). Comprehensive transposon mutant library of Pseudomonas aeruginosa. Proc. Natl. Acad. Sci. USA 100, 14339–14344. 10.1073/pnas.2036282100. [PubMed: 14617778]
43. Csürgő B, Leon LM, Chau-Ly IJ, Vasquez-Rifo A, Berry JD, Mahendra C, Crawford ED, Lewis JD, and Bondy-Denomy J (2020). A compact Cascade-Cas3 system for targeted genome engineering. Nat. Methods 17, 1183–1190. 10.1038/s41592-020-00980-w. [PubMed: 33077967]
44. Qiu D, Damron FH, Mima T, Schweizer HP, and Yu HD (2008). PBAD-Based Shuttle Vectors for Functional Analysis of Toxic and Highly Regulated Genes in Pseudomonas and Burkholderia spp. and Other Bacteria. Appl. Environ. Microbiol 74, 7422–7426. 10.1128/AEM.01369-08. [PubMed: 18849445]
45. Hmelo LR, Borlee BR, Almblad H, Love ME, Randall TE, Tseng BS, Lin C, Irie Y, Storek KM, Yang JJ, et al. (2015). Precision-engineering the Pseudomonas aeruginosa genome with two-step allelic exchange. Nat. Protoc 10, 1820–1841. 10.1038/nprot.2015.115. [PubMed: 26492139]
46. Karimova G, Pidoux J, Ullmann A, and Ladant D (1998). A bacterial two-hybrid system based on a reconstituted signal transduction pathway. Proc. Natl. Acad. Sci. USA 95, 5752–5756. 10.1073/pnas.95.10.5752. [PubMed: 9576956]
47. Gilchrist CLM, and Chooi Y-H (2021). clinker & clustermap.js: automatic generation of gene cluster comparison figures. Bioinformatics 37, 2473–2475. 10.1093/bioinformatics/btab007. [PubMed: 33459763]
48. Waterhouse AM, Procter JB, Martin DMA, Clamp M, and Barton GJ (2009). Jalview Version 2--a multiple sequence alignment editor and analysis workbench. Bioinforma. Oxf. Engl 25, 1189–1191. 10.1093/bioinformatics/btp033.
49. Holm L, Laiho A, Törönen P, and Salgado M (2023). DALI shines a light on remote homologs: One hundred discoveries. Protein Sci. Publ. Protein Soc 32, e4519. 10.1002/pro.4519.
50. Schrödinger. The PyMOL Molecular Graphics System, Version 2.0 (Schrödinger, LLC).
51. LaFleur TL, Hossain A, and Salis HM (2022). Automated model-predictive design of synthetic promoters to control transcriptional profiles in bacteria. Nat. Commun 13, 5159. 10.1038/s41467-022-32829-5. [PubMed: 36056029]
52. Altschul SF, Gish W, Miller W, Myers EW, and Lipman DJ (1990). Basic local alignment search tool. J. Mol. Biol 215, 403–410. 10.1016/S0022-2836(05)80360-2. [PubMed: 2231712]
53. Edgar RC (2004). MUSCLE: multiple sequence alignment with high accuracy and high throughput. Nucleic Acids Res. 32, 1792–1797. 10.1093/nar/gkh340. [PubMed: 15034147]
54. Pawluk A, Bondy-Denomy J, Cheung VHW, Maxwell KL, and Davidson AR (2014). A new group of phage anti-CRISPR genes inhibits the type I-E CRISPR-Cas system of Pseudomonas aeruginosa. mBio 5, e00896. 10.1128/mBio.00896-14. [PubMed: 24736222]
55. Huiting E, Cao X, Ren J, Athukoralage JS, Luo Z, Silas S, An N, Carion H, Zhou Y, Fraser JS, et al. (2023). Bacteriophages inhibit and evade cGAS-like immune function in bacteria. Cell 186, 864–876.e21. 10.1016/j.cell.2022.12.041. [PubMed: 36750095]
56. Ellison CK, Dalia TN, Dalia AB, and Brun YV (2019). Real-time microscopy and physical perturbation of bacterial pili using maleimide-conjugated molecules. Nat. Protoc 14, 1803–1819. 10.1038/s41596-019-0162-6. [PubMed: 31028374]

Highlights

- *P. aeruginosa* prophages express proteins resembling the type IV pilus minor pilin, FimU
- Phage FimU is incorporated into the tip of the type IV pilus without disrupting function
- Infection of phages binding the pilus tip is prevented by prophage-expressed phage FimU
- The inhibitory effects of phage FimU are specific to phages that bind to the pilus tip

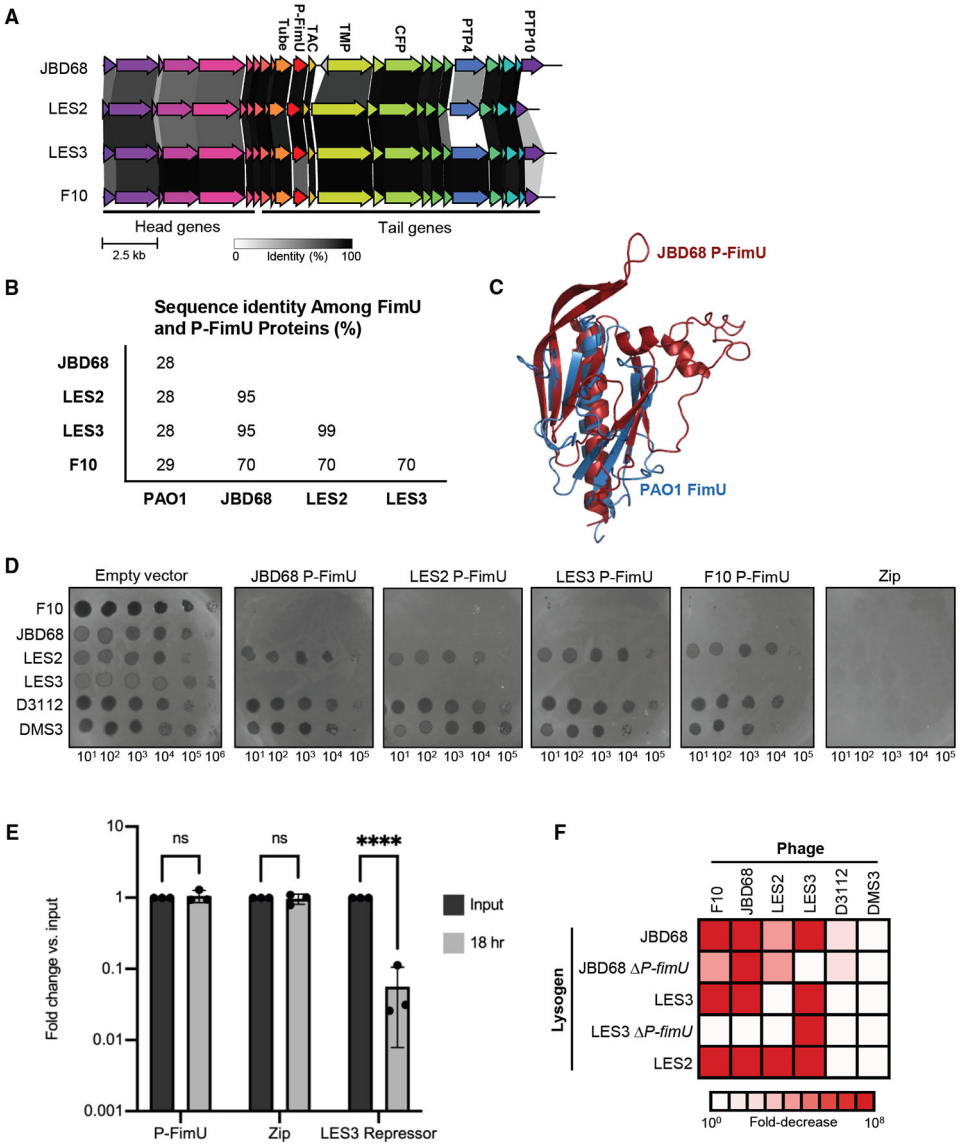

Figure 1. F10-like phages encode a protein similar to the FimU protein encoded by *Pae* strain PAO1 that inhibits replication of related phages

(A) Genomic maps of the morphogenetic regions of F10-like phages are shown. Genes encoding P-FimU proteins are indicated in red. The percent identity between homologous proteins in these phages is indicated. The functions of some conserved tail proteins are indicated: tail tube (tube), tape measure protein (TMP), tail assembly chaperone (TAC), and central fiber protein (CFP). Relevant putative tail-tip proteins are also indicated (PTP4 and PTP10).

(B) Pairwise percent identities among PAO1 FimU and P-FimU proteins.

(C) A structural overlay of PAO1 FimU (blue) and the phage JBD68 P-FimU protein (red) is shown. The P-FimU structures were predicted using AlphaFold3 and were truncated at the N terminus to match the solved structure of PAO1 FimU (PBD: 4IPU). Predicted template modeling (pTM) scores of predicted P-FimU structures are reported in Table S1.

(D) 10-fold dilutions of lysates of F10-like phages and MP22-like (DMS3 and D3112) T4P-dependent phages were spotted onto lawns of strain PAK expressing P-FimU proteins or JBD26 Zip from a high-copy-number plasmid (pHERD30T). Arabinose was added to induce gene expression.

(E) Adsorption assay of phage LES3 against *Pae* strain PAO1 expressing JBD68 P-FimU, Zip, or LES3 repressor from pHERD30T. Phages were added to cells in exponential growth at an MOI of 0.1. Phage titers were measured after 18 h of incubation. Each data point represents the average titer of phages plated in triplicate and normalized against the input titer at time 0 h, and the bar graphs indicate the mean ± SD. Statistics were conducted using an unpaired two-tailed Student's *t* test comparing phage titers normalized to input at 0 and 18 h (****$p < 0.0001$). Representative images are shown in Figure S1B.

(F) A heatmap is shown summarizing the fold decrease in plaquing efficiency observed when the indicated phages were spotted onto lysogenic strains bearing JBD68, LES2, or LES3 prophages. Prophages harboring deletion mutations in the genes encoding the P-FimU proteins were also tested. Representative phage spotting plates corresponding to this experiment are shown in Figure S1C.

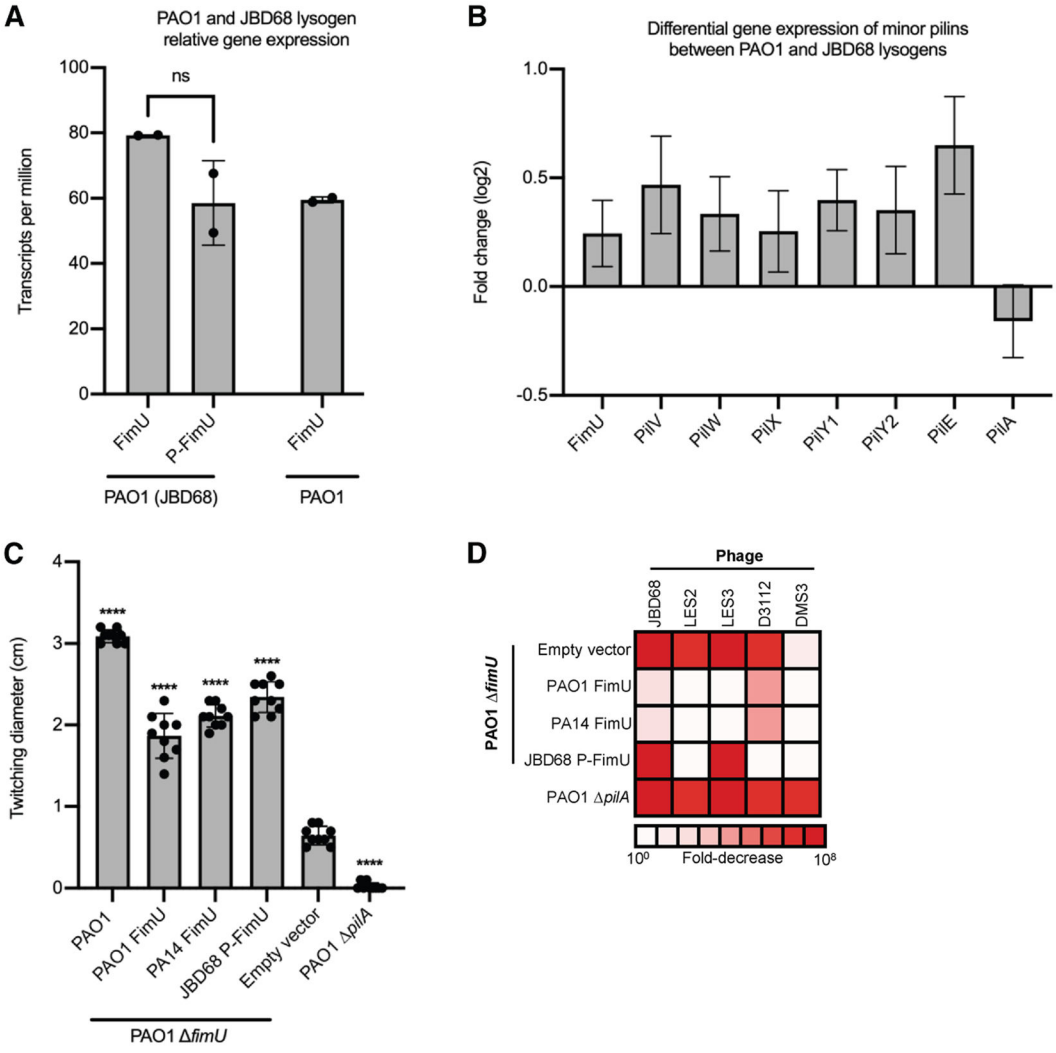

Figure 2. P-FimU proteins are likely regulated in a manner similar to bacterial FimU and restore T4P activity in the absence of bacterial FimU

(A) Transcripts per million counts of bacterial *fimU* and JBD68 *p-fimU* are shown as determined by RNA-seq analysis of PAO1 and a PAO1 JBD68 lysogen. Individual data points represent transcripts per million of two biological replicates, and the bar graphs indicate the mean ± SD. ns, non-significant by unpaired two-tailed Student's *t* test comparing transcripts per million of *fimU* and *p-fimU*.

(B) Differential gene expression analysis (DESeq2) of minor pilin genes and *pilA* between PAO1 and PAO1 JBD68 lysogens. Bar graphs indicate the mean ± SD.

(C) The twitching diameters of PAO1 Δ*fimU* strains expressing JBD68 P-FimU and bacterial FimU proteins from pHERD30T. Individual data points represent the twitching diameter of 9 biological replicates, and the bar graphs indicate the mean ± SD. Each condition was compared to PAO1 Δ*fimU* expressing an empty vector with one-way ANOVA using multiple comparisons, ****$p < 0.0001$.

(D) Heatmap representing the fold decrease in plaquing efficiency relative to that on wild-type PAO1 of the indicated phages on lawns of a PAO1 Δ*fimU* strain expressing JBD68

P-FimU and bacterial FimU proteins from pHERD30T. Representative full plates for these experiments are shown in in Figure S2C.

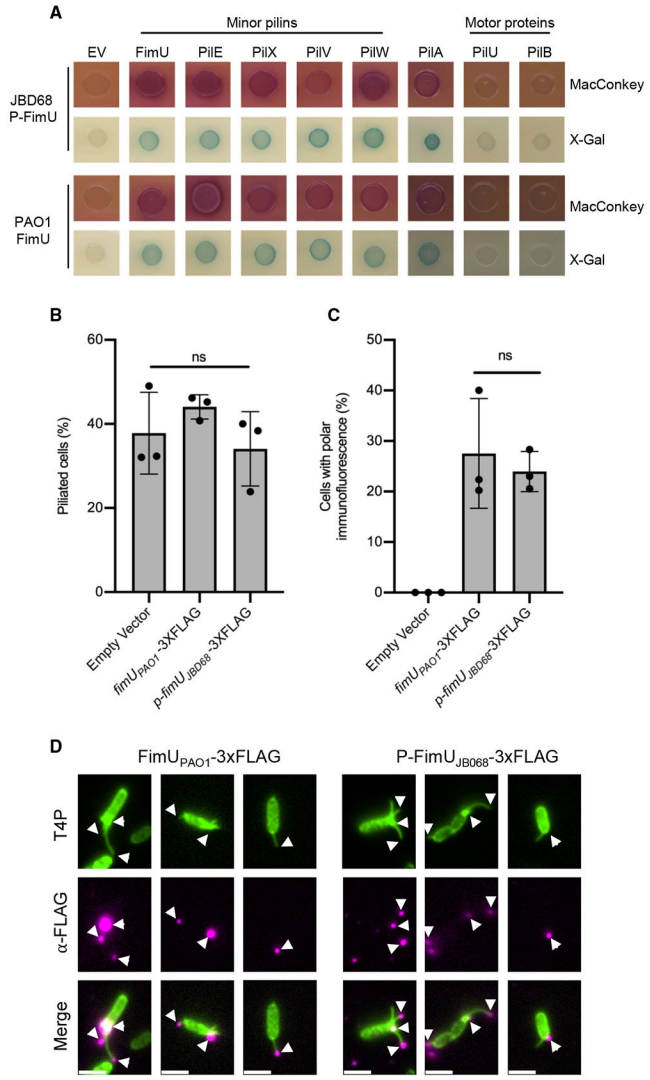

Figure 3. JBD68 P-FimU is incorporated into *P. aeruginosa* T4P

(A) BacTH assays were performed by co-expressing JBD68 P-FimU or *Pae* strain PAO1 FimU (T25 fusion) with the minor pilin proteins, PilA, and T4P motor proteins PilU and PilB (T18 fusion). Interactions were detected by spotting cells on X-Gal and MacConkey maltose agar.

(B) Percentage of cells making T4P in indicated strains as detected by fluorescence microscopy is shown. Each data point represents a biological replicate, and the bar graphs indicate the mean ± SD. Statistics were determined by Tukey's multiple comparisons test.

(C) Percentage of cells with polar immunofluore-scence signal in the indicated strains is shown. Each data point represents a biological replicate, and the bar graphs indicate the mean ± SD. Statistics were determined using Student's *t* test. ns, not significant.

(D) Fluorescence microscopy images of cells from populations of indicated strains are shown with immunolabeled FimU and P-FimU (magenta) associated with T4P (green) labeled with AF488-maleimide. Arrows indicate pole- and pilus-associated FimU. Scale bars, 2 μm.

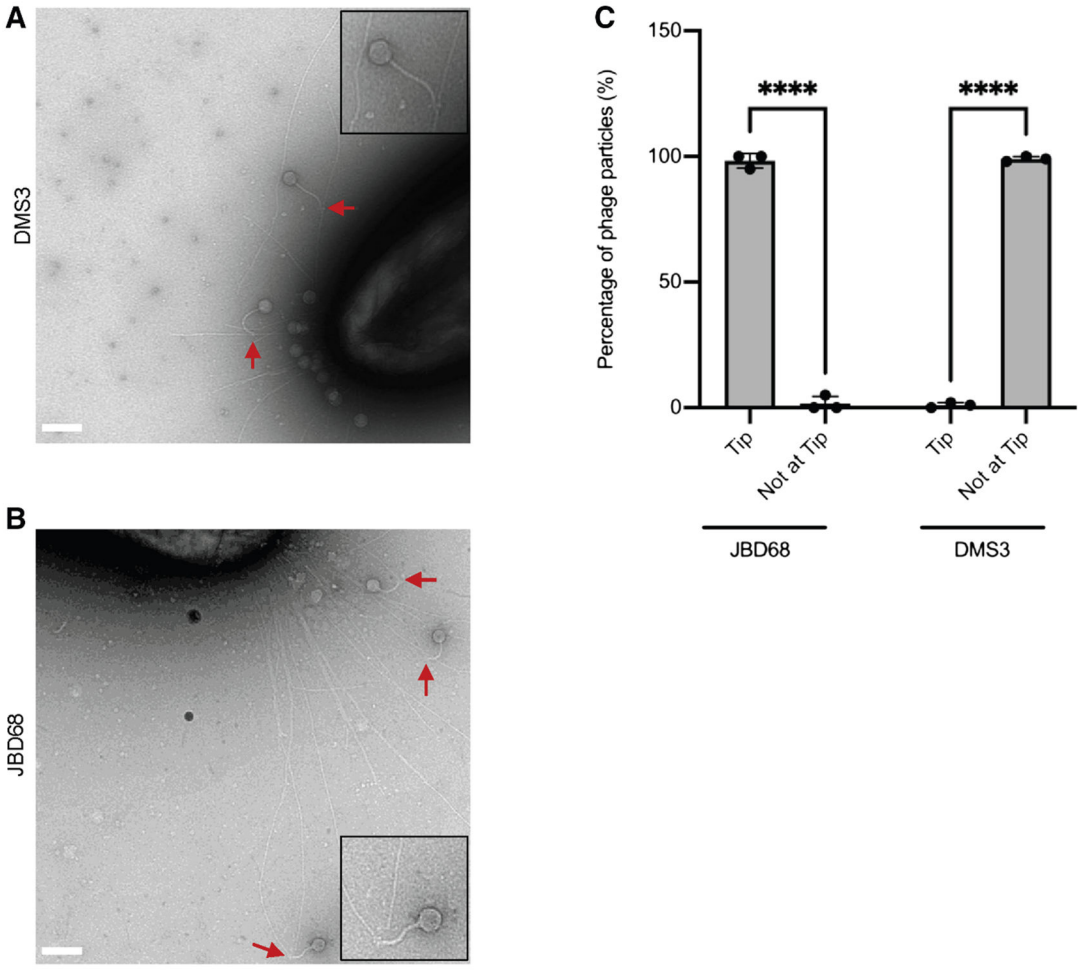

Figure 4. F10-like phages bind to the tip of the T4P

(A and B) Negatively stained transmission electron micrographs of phages DMS3 (A) and JBD68 (B) interacting with the T4P of the *Pae* strain PAO1. Interaction is indicated by red arrows. Images were taken at various magnifications to maximize the number of phages in the field of view. Scale bars, 200 nm. Additional views of phages binding to the T4P are shown in Figure S3C.

(C) The percentage of JBD68 and DMS3 particles bound at different locations of the T4P. Individual data points represent the percentage of 100 clearly visible phages bound to the pilus away from the cell body for 3 replicate grids for each phage, and the bar graphs indicate the mean ± SD. Statistics were performed using an unpaired two-tailed Student's *t* test comparing phages bound at the tip and not at the tip for both DMS3 and JBD68 (****$p < 0.0001$).

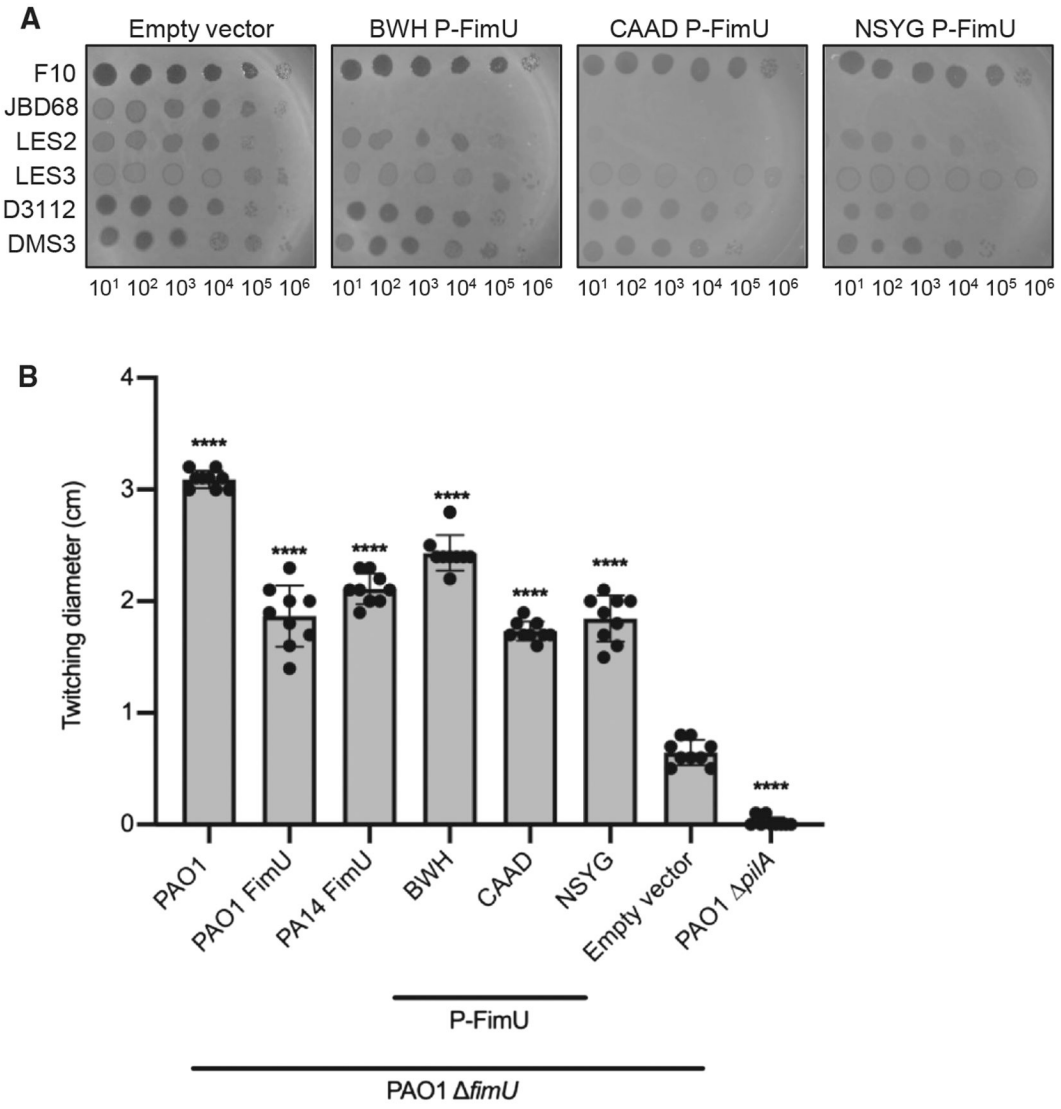

Figure 5. Diverse P-FimU proteins block F10-like phages without disrupting T4P activity

(A) 10-fold dilutions of lysates of F10-like phages and non-F10-like T4P-dependent phages (D3112 and DMS3) were spotted onto lawns of strain PAK expressing the indicated P-FimU protein from a high-copy-number plasmid (pHERD30T).

(B) The twitching diameters of PAO1 Δ*fimU* strains expressing the indicated P-FimU protein and bacterial FimU proteins from pHERD30T are shown. Individual data points represent the twitching diameter of 9 biological replicates, and the bar graphs indicate the mean ± SD. Each condition was compared to PAO1 Δ*fimU* expressing an empty vector with one-way ANOVA using multiple comparisons, ****$p < 0.0001$.

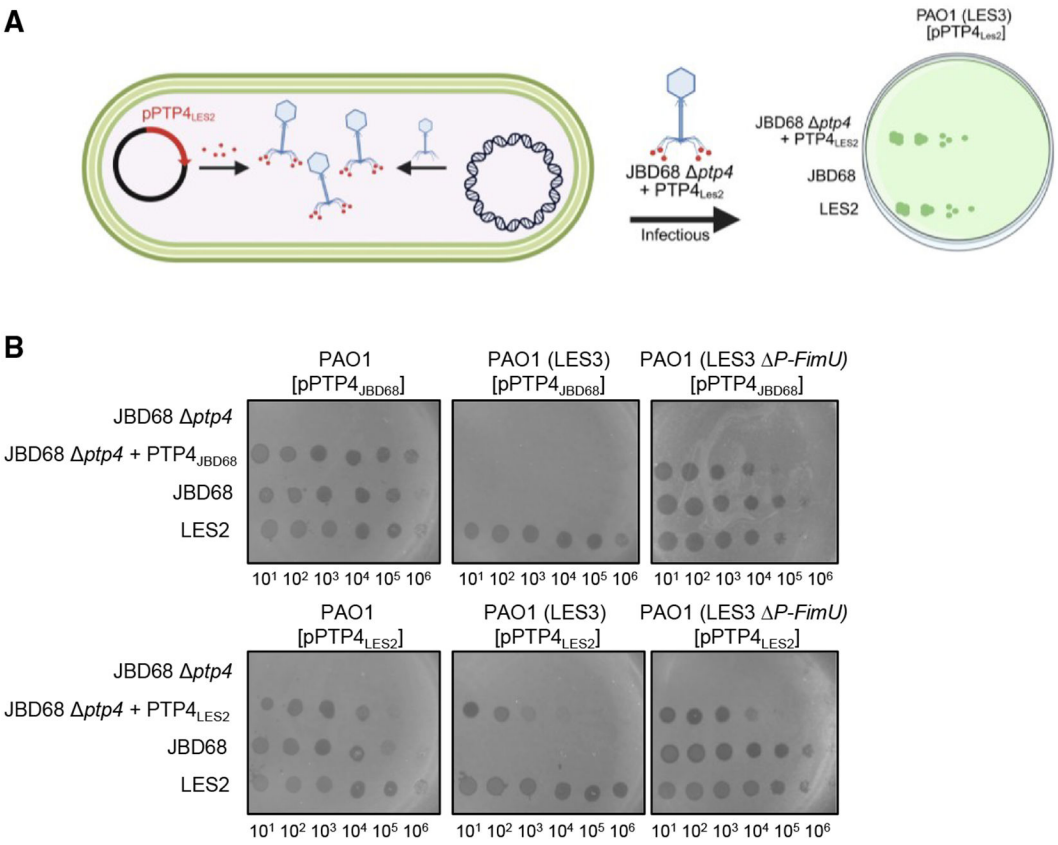

Figure 6. Swapping F10-like PTP4 overcomes inhibition by P-FimU expressed from the LES3 prophage

(A) A schematic of the JBD68 Δ*ptp4* complementation experiment is shown. JBD68 Δ*ptp4* prophages were induced in cells containing a plasmid containing an empty vector (EV) or plasmids expressing $PTP4_{JBD68}$ or $PTP4_{LES2}$. The resulting lysate was then plated on cells containing the plasmids expressing $PTP4_{JBD68}$ or $PTP4_{LES2}$ ([$pPTP4_{JBD68}$] or [$pPTP4_{LES2}$], respectively).

(B) 10-fold dilutions of lysates of phage JBD68 Δ*ptp4* complemented with the indicated PTP4 proteins were spotted onto lawns of the indicated strains. The prophages contained in these strains are indicated in parentheses. The indicated PTP proteins were expressed from a plasmid.

KEY RESOURCES TABLE

REAGENT or RESOURCE	SOURCE	IDENTIFIER
Antibodies		
Mouse α-FLAG antibody (monoclonal)	Sigma	Cat# F3165; RRID: AB_259529
Goat α-mouse-AF555	Abcam	Cat# AB150078; RRID:AB272519
Bacterial and virus strains		
P. aeruginosa PAO1	A. Davidson Lab	GenBank: NC_002516.2
P. aeruginosa PAK	A. Davidson Lab	GenBank: LR657304.1
P. aeruginosa PAK (JBD68)	A. Davidson Lab	N/A
P. aeruginosa PAK (LES2)	A. Davidson Lab	N/A
P. aeruginosa PAK (LES3)	A. Davidson Lab	N/A
P. aeruginosa PAK (JBD68 Δ*p-fimU*)	A. Davidson Lab	N/A
P. aeruginosa PAK (LES3 Δ*p-fimU*)	A. Davidson Lab	N/A
P. aeruginosa PAO1 Δ*fimU*	A. Davidson Lab[16]	N/A
P. aeruginosa PAO1 Δ*pilA*	A. Davidson Lab[42]	N/A
P. aeruginosa PAO1 Δ*pilT*	A. Davidson Lab[42]	N/A
P. aeruginosa PAO1 I-C CRISPR	A. Davidson Lab[43]	N/A
P. aeruginosa PAO1 I-C CRISPR *Δhel*	A. Davidson Lab	N/A
P. aeruginosa PAO1 *pilA* A86C, *pilT*::Tn5	C. Ellison Lab[21]	N/A
E. coli DH5α	A. Davidson Lab	N/A
E. coli SM10 λpir	A. Davidson Lab	N/A
E. coli BTH101	A. Davidson Lab[32]	N/A
P. aeruginosa phage JBD68	A. Davidson Lab	GenBank: KY707339.1
P. aeruginosa phage JBD68 Δ*p-fimU*	A. Davidson Lab	N/A
P. aeruginosa phage JBD68 Δ*ptp4*	A. Davidson Lab	N/A
P. aeruginosa phage JBD68 Δ*ptp10*	A. Davidson Lab	N/A
P. aeruginosa phage F10	A. Davidson Lab	GenBank: NC_007805.1
P. aeruginosa phage LES2	A. Davidson Lab	N/A
P. aeruginosa phage LES3	A. Davidson Lab	N/A
P. aeruginosa phage LES3 Δ*p-fimU*	A. Davidson Lab	N/A
P. aeruginosa phage DMS3	A. Davidson Lab	GenBank: NC_008717.1
P. aeruginosa phage D3112	A. Davidson Lab	GenBank: AY394005.1
P. aeruginosa phage M6	A. Davidson Lab	GenBank: NC_007809.1
P. aeruginosa phage F116	A. Davidson Lab	GenBank: NC_006552.1
P. aeruginosa phage Luz19	A. Davidson Lab	GenBank: NC_010326.1
P. aeruginosa phage AB05	A. Davidson Lab	GenBank: NC_026602.1
P. aeruginosa phage ΦKMV	A. Davidson Lab	GenBank: NC_005045.1
P. aeruginosa phage ΦKMZ	A. Davidson Lab	N/A
Chemicals, peptides, and recombinant proteins		
Tris	Bioshop	Cat# TRS003
Sodium chloride	Bioshop	Cat# SOD004
BioTryptone	BioBasic	Cat# TG217

REAGENT or RESOURCE	SOURCE	IDENTIFIER
Magnesium sulfate (heptahydrate)	BioBasic	Cat# M5BO329
L−(+)Arabinose	Bioshop	Cat# ARB222.100
Phosphate buffered saline	Bioshop	Cat# PBS408
Tween 20	Bioshop	Cat# TWN508
Agar	Bioshop	Cat# AGR100.500
Ultra Pure Agarose	Invitrogen	Cat# 16500_500
Difco MacConkey Agar Base	BD	Cat# 281810
Difco Maltose	BD	Cat# 216830
X-Gal	Biobasic	Cat# BB0083
Mitomycin C	Cell Signaling Technologies	Cat# 51854S
NcoI-HF	New England Biolabs	Cat# R3193S
EcoRI-HF	New England Biolabs	Cat# R3101S
HindIII-HF	New England Biolabs	Cat# R3104S
KpnI-HF	New England Biolabs	Cat# R3142S
XbaI-HF	New England Biolabs	Cat# R0145S
BsaI-HF v2	New England Biolabs	Cat# R3733S
T4 DNA Ligase	New England Biolabs	Cat# M0202S
T4 Polynucleotide Kinase	New England Biolabs	Cat# M0201S
T4 DNA Ligase Buffer	New England Biolabs	Cat# B0202A
DpnI	ThermoFisher	Cat# ER1705
Uranyl acetate	Electron Microscopy Sciences	Cat# 22400
Gentamycin sulfate	Bioshop	Cat# GTA401
Ampicillin	Bioshop	Cat# AMP201
Kanamycin	Bioshop	Cat# KAN201
AF488-maleimide	ThermoFisher	Cat# A10254
Crystal violet	Bioshop	Cat# CRY422.25
Carbon-coated TEM grids	Electron Microscopy Sciences	Cat# CF150-Cu
Deposited data		
PAO1 and PAO1 (JBD68) RNA-Seq raw reads	This study	SRA: PRJNA1364051
Recombinant DNA		
pHERD30T	Qiu et al.[44]	N/A
pEX18Gm	Hmelo et al.[45]	N/A
pKT25	Karimova et al.[46]	N/A
pUT18C	Karimova et al.[46]	N/A
PAO1 FimU	This study	N/A
PA14 FimU	This study	N/A
JBD68 P-FimU	This study	N/A
Les P-FimU	This study	N/A
F10 P-FimU	This study	N/A
BWH P-FimU	This study	N/A
CAAD P-FimU	This study	N/A
NSYG P-FimU	This study	N/A

REAGENT or RESOURCE	SOURCE	IDENTIFIER
Zip	Taylor et al.[9]	N/A
LES3 Repressor	This study	N/A
JBD68 P-FimU 3xFLAG	This study	N/A
PAO1 FimU 3xFLAG	This study	N/A
$pPTP4_{JBD68}$	This study	N/A
$pPTP4_{LES2}$	This study	N/A
T25 JBD68 P-FimU	This study	N/A
T25 F10 P-FimU	This study	N/A
T25 PAO1 FimU	This study	N/A
T25 PAO1 FimS	This study	N/A
T18 PAO1 FimS	This study	N/A
T18 PAO1 PilA	This study	N/A
T18 PAO1 PilE	Marko et al.[31]	N/A
T18 PAO1 PilX	Marko et al.[31]	N/A
T18 PAO1 PilV	Marko et al.[31]	N/A
T18 PAO1 PilW	Marko et al.[31]	N/A
T18 PAO1 PilU	Marko et al.[31]	N/A
T18 PAO1 PilB	Marko et al.[31]	N/A
Oligonucleotides		
PAO1 *fimU* F: AAACCATGGCCTC ATATCGTTCCAACTCGACCGG	Eurofins Genomics	NcoI
PAO1 *fimU* R: AAAAAGCTTTCAA TAGCATGACTGGGGCGC	Eurofins Genomics	HindIII
PA14 *fimU* F: AAACCATGGCCC GCTCTATTTGTCGCAGCGCC	Eurofins Genomics	NcoI
PA14 *fimU* R: AAAAAGCTTTCA GTTACAGCTGTCCGGTTGCTTTG	Eurofins Genomics	HindIII
JBD68 *p-fimU* F: AAACCATGGCC TACTCTAGGTCGCGCGGATTTACC	Eurofins Genomics	NcoI
JBD68 *p-fimU* R: AAAAAGCTTTC AGCAGCCAGAAGCGTCCC	Eurofins Genomics	HindIII
F10 *p-fimU* F: AAACCATGGCCTA CTCTAGGTCGCGCGGATTTA	Eurofins Genomics	NcoI
F10 *p-fimU* R: AAAAAGCTTCTAAC AGTCAAAAGTATCCCAGGATTCC	Eurofins Genomics	HindIII
LES3 *p-fimU* F: AAACCATGGCCTA CTCTAGGTCGCGCGGATTTACC	Eurofins Genomics	NcoI
LES3 *p-fimU* R: AAAAAGCTTTCAG CAGCCAGAAGTGTCCCA	Eurofins Genomics	HindIII
BWH *p-fimU* F: AAACCATGGCC GGCTCCAAG	Eurofins Genomics	NcoI
BWH *p-fimU* R: AAAAAGCTTCTAA CTGGGTTTTACAGCGCAGGc	Eurofins Genomics	HindIII
CAAD *p-fimU* F: AAACCATGGGTT GAAATGTACTCTAGGTCGCGCG	Eurofins Genomics	NcoI
CAAD *p-fimU* R: AAAAAGCTTTCAG GTTGGTTTCTTGGCGCA	Eurofins Genomics	HindIII

REAGENT or RESOURCE	SOURCE	IDENTIFIER
NSYG *p-fimU* F: AAACCATGGATTC GCATAAATCAAGCTCAGCGTGG	Eurofins Genomics	NcoI
NSYG *p-fimU* R: AAAAAGCTTCTAT TGGTCCTTGGCACACTGTG	Eurofins Genomics	HindIII
LES3 repressor F: AAACCATGGCCA TCGATATCACGACAATCCGCCGCGCGA AC	Eurofins Genomics	NcoI
LES3 repressor R: AAAAAGCTTTCAG TGTCGCCGCCGGCGCA	Eurofins Genomics	HindIII
JBD68 *p-fimU* 3xFLAG F: TATAAAGAT CATGATATTGATTATAAAGATGATGAT GATAAATGAAAGCTTGGCACTGGCCG	Eurofins Genomics	Restriction free
JBD68 *p-fimU* 3xFLAG R: ATCACCATC ATGATCTTTATAATCTCCACCACTTCC ACCTGCGCAGCCAGAAGCGTCCCAAG	Eurofins Genomics	Restriction free
PAO1 *fimU* 3xFLAG F: TATAAAGATCA TGATATTGATTATAAAGATGATGATGA TAAATGAAAGCTTGGCACTGGCCG	Eurofins Genomics	Restriction free
PAO1 *fimU* 3xFLAG R: ATCACCATCAT GATCTTTATAATCTCCACCACTTCCAC CTGCATAGCATGACTGGGGCGCCT	Eurofins Genomics	Restriction free
JBD68 *p-fimU* T25 F: AAATCTAGAGAT GTACTCTAGGTCGCGCGGAT	Eurofins Genomics	XbaI
JBD68 *p-fimU* T25 R: AAAGGTACCTC AGCAGCCAGAAGCGTCCC	Eurofins Genomics	KpnI
F10 *p-fimU* T25 F: AAACTGCAGGGAT GTACTCTAGGTCGCGCGGAT	Eurofins Genomics	PstI
F10 *p-fimU* T25 R: AAAGGTACCCTAA CAGTCAAAAGTATCCCAGGATTCCTCT	Eurofins Genomics	KpnI
PAO1 *fimU* T25 F: AAATCTAGAGATG TCATATCGTTCCAACTCGACCG	Eurofins Genomics	XbaI
PAO1 *fimU* T25 R: AAAGAATTCTCAA TAGCATGACTGGGGCGC	Eurofins Genomics	EcoRI
PAO1 *pilA* 18C F: AAATCTAGAGATGA AAGCTCAAAAAGGCTTTACCTTGATCG	Eurofins Genomics	XbaI
PAO1 *pilA* 18C R: AAAGAATTCTTAGT TATCACAACCTTTCGGAGTGAACATC	Eurofins Genomics	EcoRI
PAO1 *fimS* B2 *F*: AAATCTAGAGATGC CTATCCGATTCAAGCCCG	Eurofins Genomics	XbaI
PAO1 *fimS* B2 R: AAAGAATTCTCAGG CTTCCTGCATGAGTCG	Eurofins Genomics	EcoRI
JBD68 *ptp4* F: AAAGAATTCATGGCT CTTTCAGATGAGCGC	Eurofins Genomics	EcoRI
JBD68 *ptp4* R: AAAAAGCTTTCAAAC GTAGGAATAGAAAGCGTTCG	Eurofins Genomics	HindIII
LES2 *ptp4* F: AAAGAATTCATGGCT CTATCAGATGAGCGC	Eurofins Genomics	EcoRI
LES2 *ptp4* R: AAAGGTACCTCAAAC GTAGGAATAGAAAGCGCT	Eurofins Genomics	KpnI
LES3 *p-fimU* I-C spacer F: GAAACTG GCTGTGTTGTGTTTGCTTACAATGG TTCAATAG	Eurofins Genomics	BsaI
LES3 *p-fimU* I-C spacer R: GCGACT ATTGAACCATTGTAAGCAAACACA ACACAGCCAG	Eurofins Genomics	BsaI

REAGENT or RESOURCE	SOURCE	IDENTIFIER
JBD68 *p-fimU* I-C spacer F: GAAAC CGTCGTTTGTGAATCTCATAAAAG GCAATAGCATG	Eurofins Genomics	BsaI
JBD68 *p-fimU* I-C spacer R: GCGA CATGCTATTGCCTTTTATGAGATT CACAAACGACGG	Eurofins Genomics	BsaI
JBD68 *ptp10* I-C spacer F: GAAAC CGTCGTTTGTGAATCTCATAAAAG GCAATAGCATG	Eurofins Genomics	BsaI
JBD68 *ptp10* I-C spacer R: GCGAC ATGCTATTGCCTTTTATGAGATTC ACAAACGACGG	Eurofins Genomics	BsaI
Software and algorithms		
Clinker	Gilchrist and Chooi[47]	https://github.com/gamcil/clinker
Jalview 2	Waterhouse et al.[48]	https://www.jalview.org
AlphaFold3	Jumper et al.[28]	https://alphafoldserver.com/welcome
DALI	Holm et al.[49]	http://ekhidna2.biocenter.helsinki.fi/dali/
Pymol 3	Schrödinger[50]	https://pymol.org
Biorender	N/A	https://www.biorender.com
De Novo DNA	LaFleur et al.[51]	https://salislab.net/software/predict_promoter_calculator
GraphPad Prism 9 & Prism 10	N/A	https://www.graphpad.com
NIS-Elements Imaging	N/A	https://www.microscope.healthcare.nikon.com/products/software/nis-elements/software-resources
Critical commercial assays		
GenepHIowTM Gel/PCR Kit	FroggaBio Scientific Solutions	Cat# DFH300
EZ-10 Spin Column Plasmid DNA Minipreps Kit	BioBasic	Cat# BS614
Illumina® Ribo-Zero Plus rRNA Microbiome depletion kit	Illumina	Cat# 20072062
PhusionTM High-Fidelity DNA Polymerase	ThermoFisher	Cat# F530S